Effects of color screening in hadron–nucleus interactions

B. Z. Kopeliovich

Joint Institute for Nuclear Research, Dubna

Fiz. Elem. Chastits At. Yadra **21**, 117–171 (January–February 1990)

The possibility of studying color dynamics in strong interactions at high energies through hadron scattering by nuclei is discussed. Various manifestations of the "color" transparency of nuclei, i.e., the decrease in the absorption in the nuclear medium of compressed hadronic configurations, are considered. The color structure of the Pomeron in the case of hadron–nucleus scattering leads to new corrections to the Glauber approximation, and also to the possibility of the formation of induced color dipoles in nuclei. The space–time picture of the screening of color charges, i.e., hadronization, leads to nontrivial nuclear screening of both hard processes (production of J/Ψ and of hadrons with large p_T) and soft processes (inclusive production of hadrons with $x_F \to 1$). A decrease in the absorption of particles in the case of tunneling from the vacuum in the presence of a nuclear medium is found. A mechanism of below-threshold production of hadrons in multiquark configurations in nuclei is proposed.

INTRODUCTION

Interactions of high-energy hadrons with nuclei are traditionally used to obtain information about the space–time structure of hadron interactions and about the nature of the nuclear forces. Often, this information is unique. In hadron–hadron interactions the reaction products are detected at asymptotically large distances, much greater than the scales characteristic of the strong interactions. The only way in which the properties of incompletely formed hadronic states can be studied is evidently through scattering by a second target. Since the secondary scattering must occur within the time characteristic of strong interactions, of the order of 1 F, it is necessary to use a nucleus, which is treated here as a collection of nucleon targets.

Unfortunately, conclusions can usually be drawn about the dynamics of the processes only on the basis of very indirect indications. As a rule, the experimental information takes the form of a dependence on the atomic number A of the nucleus. Therefore, this branch of research is often called A^α physics.

Although attempts at a rigorous description of peripheral or, as they are called, "soft" hadronic processes in quantum chromodynamics (QCD) encounter the unresolved large-distance problem, there are various phenomenological models which use the ideas of QCD and which, under certain simplifications, permit an understanding of the main features of these processes. Thus, the hadron wave functions can be described in potential models, bag models, string models, etc. For what follows, it is important that in all these models the hadron is a colorless object with hidden color. The mutual screening of the color of the various constituents of the hadron leads to a significant dependence of the interaction cross section on the rms radius of the hadron.[1] Point colorless states should not interact at all. This is one of the basic and model-independent consequences of QCD. As regards its experimental verification, model calculations[1] confirm a very precise correspondence between the hierarchies of the radii of the hadrons and of the cross sections of their interaction. Nevertheless, these results cannot be regarded as a convincing confirmation of the predictions of QCD, since hadrons that have different radii also have different quark compositions. This last circumstance enables one to reproduce the cross sections equally in a "colorless" model of the quark constituents by introducing different cross sections for the interaction of the various quark species. It would appear that it is only by the use of nuclear targets that one can set up a critical experiment and obtain convincing proof that compressed hadronic configurations have small interaction cross sections. This question is considered in detail below.

The color-confinement problem is solved in the models by vacuum instability and screening of distant color charges through the tunneling production of quark–antiquark or gluon pairs from the vacuum. The most popular version of this approach is the model of a chromoelectric tube[2,3] or string, which is constructed by analogy with the bag model. Suppose that the vacuum energy density has a jump B at the boundary of a region within which a field of color charges, which suppresses the vacuum fluctuations, is localized. Requiring a minimum of the total energy, we can easily show that the field between two distant color charges (that form a color singlet) takes the equilibrium shape of a tube of constant cross section. The tube radius is $R^4 = g^2/8\pi^2 B$, and the energy density of the field per unit length of the tube is $\varkappa = g(B/8)^{1/2}$, where g is the color charge at the ends of the tube. If the longitudinal dimension of the tube is appreciably greater than the transverse dimension, the tube can be regarded as a one-dimensional string. Such a field configuration corresponds to a linearly rising potential $V = \varkappa r$, which, in its turn, guarantees linearity of the Regge trajectories, and the value $\varkappa$ is related to the universal slope parameter $\alpha'_R \approx 0.9$ GeV^2 of the Regge trajectories:

$$\varkappa = (2\pi\alpha'_R)^{-1} \approx 1 \text{ GeV/F}.$$

It should be noted that the string is very unstable—it can readily "snap" because the field stimulates production from the vacuum of quark–antiquark pairs, which completely screen the string field. The pair production mechanism is analogous to the Schwinger phenomenon in electrodynamics, the production of electron–positron pairs in an external electric field. It can readily be understood as a tunneling effect, since the production of quark pairs becomes energetically advantageous if they are formed at relative separation $l > 2m_q/\varkappa$, where m_q is the quark mass. We shall not use Schwinger's formula to estimate the probability of pair production, since the conditions for its validity are strongly vio-

 0090-4759/90/010049-25$04.00

lated in the case of a color string (for example, the field of the produced quarks strongly disturbs the external field). Instead of this, we introduce a parameter W, the probability density for production of a pair during unit time for unit length of the string. Analysis of the data on e^+e^- annihilation indicates that $W \approx 2\ \mathrm{F}^{-2}$. This means that it is difficult to stretch the string to a length appreciably greater than 1 F—it snaps [1].

Indeed, it is snappings of strings that are in this model the main source of hadronization. The energy needed to produce the hadrons appears by virtue of the stopping of the color charge at the end of the string by the string tension: $\dot{p} = -\varkappa$. It should be noted that the coefficient of the string tension that arises as a result of the color charge exchange and subsequent hadronization may differ from (exceed) the value for the static solution, for example, because of bremsstrahlung of soft gluons. Therefore, $\varkappa_{\text{eff}}$ must also be regarded as unknown.

Below we give examples of how it is possible to test in hadron–nucleus processes our ideas about the space–time picture of hadronization and the chronology of hadron production and find the effective parameters of the color string from an analysis of experimental data. We also obtain additional information about the exotic components of the nuclear wave functions—multiquark configurations.

The review is arranged as follows.

In Sec. 1 we give an introduction to the theory of the inelastic corrections to the Glauber–Sitenko approximation. The computational scheme and the physical nature of the inelastic corrections are explained, both in a basis of physical states, i.e., eigenstates of the free Hamiltonian, and in the basis of interaction eigenstates.

Section 2 is devoted to realization of the eigenstate method for calculating the inelastic corrections in QCD. The most striking consequence of this treatment is the existence in hadrons of passive components, for which the nuclear medium is transparent. These are the compressed hadronic configurations, which possess a small color dipole moment. We consider a number of specific examples: coherent regeneration of K_s mesons on nuclei, quasielastic scattering and quasifree charge exchange of hadrons on nuclei, and inclusive production of particles in the three-Reggeon region. The most definite manifestation of color screening is the appreciable increase in the nuclear transparency found in the $\pi^- \to \pi^0$ charge-exchange process on nuclei.

In Sec. 3 we consider the effects of multiquark color charge exchanges in nuclei, which differ fundamentally from the usual colorless multiple rescatterings characteristic of the Glauber–Sitenko approximation. Comparison of the data with elastic pd scattering yields bounds on the radius of the six-quark bag in the S^6 state. The multiple color charge exchanges induce in a nucleus color dipoles, which are dibaryonic resonances. We find the mass spectrum and decay widths of the resonances, the cross section for their production, and the contribution to the process of cumulative production of protons.

Section 4 is devoted to a traditional field of application of nuclear targets—the study of the space–time structure of the strong interactions. We show that "hard" processes such as the production of J/ψ mesons are screened in the nucleus near the kinematic boundary by soft interactions.

We consider the process of color screening when protons are hadronized in a nuclear medium. We show that, in contrast to the common point of view, the parton fragmentation length tends to zero for hadrons produced with maximal momentum. A manifestation of this effect is considered in the processes of production on nuclei of symmetric pairs of hadrons with large x_T and of the soft production of hadrons with $x_F \to 1$.

We show that the absorption is greatly weakened for below-barrier tunneling in the presence of a nuclear medium. This effect may explain the enhanced yield of slow antiprotons on nuclear targets.

At the end of the section we consider below-threshold production of hadrons on multiquark configurations in nuclei. Making a comparison with data on the production of K^+ mesons, we find upper bounds on the admixture of multiquark clusters.

1. INELASTIC CORRECTIONS TO THE EIKONAL APPROXIMATION

1.1. Inelastic intermediate states

The description of nuclear reactions at high energies is based on the Glauber–Sitenko[5] approximation. Indeed, the existence of new physical effects is usually deduced from the deviation of the results of measurements from calculations in that approximation. An extensive literature[6–10] has been devoted to the inelastic corrections to the Glauber–Sitenko approximation for the amplitude for hadron–nucleus scattering. Formally, these corrections appear as allowance for inelastic intermediate states in the diagrams shown in Fig. 1. An expression for estimating the inelastic corrections for arbitrary nuclei, corresponding to diagrams of the type of Fig. 1a, was obtained by Karmanov and Kondratyuk:[10]

$$\Delta_{\text{in}}\sigma_{\text{tot}}^{hA} = 4\pi \int d^2\mathbf{b} \int dM^2 \frac{d^2\sigma}{dM^2\, d\mathbf{q}_T^2}\Big|_{\mathbf{q}_T^2=0} e^{-\frac{1}{2}\sigma_{\text{tot}}^{hN}T(\mathbf{b})} |F(q_L, \mathbf{b})|^2. \quad (1)$$

Here σ_{tot}^{hA} and σ_{tot}^{hN} are the total cross sections for the interaction of a hadron with a nucleus and with a nucleon; $d^2\sigma/dM^2 d\mathbf{q}_T^2$ is the cross section for diffraction dissociation[8,9] with production of a mass M and transverse momentum transfer $\mathbf{q}_t$; $F(q_L\ \mathbf{b})$ is the nuclear form factor

$$F(q_L, \mathbf{b}) = \int_{-\infty}^{\infty} dz \rho(\mathbf{b}, z) e^{iq_L z}, \quad (2)$$

where $\mathbf{b}$ and z are the impact parameter and the longitudinal coordinate; $\rho(b, z)$ is the distribution function of the nuclear density; $q_L = (M^2 - m_h^2)/2E$; E is the initial energy: and $T(\mathbf{b})$ is the nuclear profile function, $T(\mathbf{b}) = F(0, \mathbf{b})$ [a more accurate expression is given in Eq. (10)]. In Eq. (1) it is

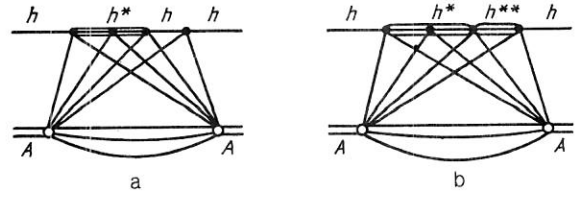

FIG. 1. Graphs corresponding to inelastic corrections.

assumed that the scattering cross sections of the ground state of the hadron and of the excited states are equal.

With increasing energy the inelastic corrections (1) increase, since q_L decreases. The inelastic corrections occur in the total cross section with a negative sign. This corresponds to an increase in the nuclear transparency, an effect that is readily understood; for allowance for inverse transitions from excited states to the initial state increase the probability for passing through the nucleus. We shall show below that in some nuclear reactions the inelastic corrections can, instead, decrease the nuclear transparency.

In the frame of reference in which the nucleus is incident on the hadron at rest, the inelastic corrections appear as allowance for fusion of the parton clouds of the nucleons[11] that are situated at the same impact parameter in the soft part of the momentum spectrum. The decrease in the number of slow partons naturally leads to a decrease in σ_{tot}^{hA}.

Although allowance for the inelastic corrections by means of the expression (1) satisfactorily describes the experimental data[12,13] for σ_{tot}^{hA}, this is due to the fact that the inelastic corrections themselves are small—a few percent. If the accuracy of the data and the calculations is increased,[14,15] it is necessary to take into account the inelastic corrections of higher order, for example, those corresponding to the graph in Fig. 1b. The same problem also arises in specific channels of nuclear reactions, where, as will be shown below, the inelastic corrections reach hundreds of percent.

1.2. Eigenstate method

The eigenstate method, proposed in Refs. 16 and 17, played an important part in the clarification of the dynamics of diffraction processes.[18,19] In Refs. 20 and 21 the method was used to calculate the inelastic corrections in hadron–nucleus reactions.

The fact that hadrons can be excited in diffraction scattering, i.e., that nondiagonal transitions exist, indicates that the basis of physical states $|h\rangle$ is inconvenient for problems of the interaction of hadrons and nuclei. We choose a basis of interaction eigenstates $|k\rangle$, which are carried into themselves under the action of the operator of the scattering amplitude:

$$\hat{f}\,|\,k\,\rangle = f_k\,|\,k\,\rangle. \tag{3}$$

Here, f_k are eigenvalues of the operator $\hat{f}$.

Assuming that the basis $|k\rangle$ is orthonormal, we expand the physical states with respect to it:

$$|\,h\rangle = \sum_k C_k^h\,|\,k\rangle. \tag{4}$$

The coefficients C_k^h satisfy the relations

$$\sum_k C_k^h\,(C_k^g)^* = \delta_{hg}; \quad \sum_h C_k^h\,(C_i^h)^* = \delta_{ik}. \tag{5}$$

The amplitude of the diffraction transition $h \to g$ has the form

$$f_{gh} = \sum_k C_k^h\,(C_k^g)^*\,f_k. \tag{6}$$

From this it can be seen that nondiagonal diffraction transitions occur only when there is a difference between the amplitudes f_k.

The inelastic diffraction cross section, summed over the final states, is

$$\sigma_{DD} = \langle f_k^2\rangle - \langle f_k\rangle^2, \tag{7}$$

where the averaging over k is done with weight $|C_k|^2$.

Knowing the spectrum of the eigenstates $|k\rangle$ and the amplitudes f_k for elastic scattering by a nucleon, we can readily calculate the partial amplitude for scattering by a nucleus. Suppose that the initial energy E is sufficiently high:

$$E/\mu^2 \gg R_A, \tag{8}$$

where μ is a mass parameter, and R_A is the nuclear radius. Then the hadronic fluctuations can be regarded as "frozen," i.e., the various eigenstates $|k\rangle$ of the hadron wave function are not mixed during the time of the interaction with the nucleus. The amplitude for the interaction with the nucleus of the state $|k\rangle$ can be calculated in the Glauber–Sitenko approximation, since there are no nondiagonal transitions.

Thus, the partial amplitude for scattering of a hadron by a nucleus for given impact parameter b, $f_{el}^{hA}(\mathbf{b})$, has the form

$$f_{el}^{hA}(\mathbf{b}) = 1 - \langle \exp[-f_k T(\mathbf{b})]\rangle. \tag{9}$$

Here, $T(\mathbf{b})$ is the nuclear profile function:

$$T(\mathbf{b}) = \int_{-\infty}^{\infty} \tilde{\rho}(\mathbf{b}, z)\,dz, \tag{10}$$

$$\tilde{\rho}(\mathbf{b}, z) = \frac{1}{2\pi B}\int d^2\mathbf{b}'\rho(\mathbf{b}', z)\exp\left[-\frac{(\mathbf{b}-\mathbf{b}')^2}{2B}\right],$$

where B is the slope parameter of the cross section for elastic hN scattering, and $\rho(\mathbf{b}, z)$ is the density function of the nucleons in the nucleus, used in what follows in the Woods–Saxon parametrization.[22] Note that the optical approximation is used in (9) for clarity. In the later calculations more exact expressions with the substitution $\exp(-\sigma T) \to (1-\sigma T/A)^A$ will be used.

The difference between the expression (9) and the Glauber–Sitenko approximation is that the entire exponential, and not only its argument, is averaged over k. The difference between the two expressions represents the inelastic correction to the partial amplitude:

$$\Delta_{\text{in}}(\mathbf{b}) = \langle \exp[-f_k T(\mathbf{b})]\rangle - \exp[-\langle f_k\rangle T(\mathbf{b})]. \tag{11}$$

This expression is equivalent to allowance for all possible intermediate states in the hadron basis.[20,21] However, this result is obtained at the price that the calculation has become model-dependent, in contrast to the expression (1). The results depend on the choice of the spectrum of eigenstates and eigenvalues of the scattering amplitude. This makes the calculation less reliable, but, on the other hand, opens up the possibility of testing theoretical models.

1.3. Mixing of eigenstates

A serious problem in the eigenstate method is the allowance for the mixing of the various components of the wave function during the passage through the nucleus. In the hadron basis, this is equivalent to taking into account the longitudinal momentum transfer to the nucleus when intermediate jets are formed. We consider the connection between the two approaches for the example of the two-compo-

nent approximation and establish the observable consequences of the mixing.[23]

Suppose that the hadron states $|\alpha\rangle$ and $|\beta\rangle$ are associated with the eigenstates $|1\rangle$ and $|2\rangle$. The equation that describes the mixing of the eigenstates on the passage through the nucleus is

$$\frac{d\,|\,k\rangle}{dl} = \sum_i Q_{ki}\,|\,i\rangle, \tag{12}$$

where l is the longitudinal coordinate, and the matrix $\hat{Q}$ has the form

$$\hat{Q} = \begin{pmatrix} q+|\,C_2\,|^2 q_L - f_1\rho & -C_1C_2^* q_L \\ -C_1^* C_2 q_L & q+|\,C_1\,|^2 q_L - f_2\rho \end{pmatrix}. \tag{13}$$

Here $q_L = (m_\beta^2 - m_\alpha^2)/2E$; f_k are the eigenvalues of the amplitude for scattering (the imaginary part) on a nucleon; and ρ is the nuclear density, here assumed constant.

The amplitude for elastic scattering of a hadron $|\alpha\rangle$ by a layer of nuclear matter of thickness l is

$$-if_{\rm el}(l) = 1 - \exp\left[\frac{f_1+f_2}{2}\rho l + il\frac{q_L}{2}\right]\left\{\cos\left(\frac{\lambda l}{2}\right) - \frac{iq_L + (|\,C_2\,|^2 - |\,C_1\,|^2)\,\rho\,(f_1-f_2)}{\lambda}\sin\left(\frac{\lambda l}{2}\right)\right\}, \tag{14}$$

where

$$\lambda = \{[(|C_2|^2 - |C_1|^2)q_L + (f_2 - f_1)\rho]^2 + 4|C_1|^2|C_2|^2 q_L^2\}^{1/2}.$$

At high energies, when the mixing can be ignored, we obtain the well-known expression (9) from (14). At lower energies in the limit $q_L/f\rho \gg 1$, when the mixing of the states $|1\rangle$ and $|2\rangle$ is large, the expression (14) can be expanded with respect to the parameter $f\rho/q_L$, and we obtain

$$\begin{aligned} \operatorname{Im} f_{\rm el}(l) = 1 - \exp[-(|\,C_1\,|^2 f_1 + |\,C_2\,|^2 f_2)\rho l] \\ - \frac{\rho^2}{q_L^2}[|\,C_1\,|^2(1-|\,C_1\,|^2) f_1^2 + |\,C_2\,|^2(1-|\,C_2\,|^2) f_2^2 \\ - 2\,|\,C_1\,|^2\,|\,C_2\,|^2 f_1 f_2]\exp[-(|\,C_1\,|^2 f_1 + |\,C_2\,|^2 f_2)\rho l] \\ \times\{1 - \exp[-(|\,C_2\,|^2 - |\,C_1\,|^2)(f_2 - f_1)\rho l]\cos(q_L l)\}. \end{aligned}$$

Here, the first two terms correspond to the Glauber–Sitenko approximation. The third term is the correction for the inelastic screening, calculated in the first order in the cross section for inelastic diffraction. This correction is identical to the expression (1) if, as in Ref. 10, we assume that $f_{\rm el}^\alpha = f_{\rm el}^\beta$, i.e., $|C_1|^2 = |C_2|^2 = 0.5$. This is readily seen by using the relation (7).

It can be seen from (13) and (14) that the characteristic mixing time of the eigenstates is characterized by $1/q_L$, This is an important conclusion; it means that for the calculation of the scattering amplitude of the hadron $|\alpha\rangle$ the corrections for mixing are determined by the Lorentz factor, which depends not on the mass m_α but on the gap $m_\beta - m_\alpha$ in the mass spectrum. Indeed, the interaction eigenstates $|k\rangle$ do not have a definite mass. Thus, the mixing time in the case of scattering, for example, of a pion contains the Lorentz factor E/m_{a_1}, and not E/m_π.

It also follows from (14) that the nuclear amplitude $f_{\rm el}^\alpha(l)$ has a real part even when the nucleon amplitude is imaginary. The reason why the real part appears is readily understood in the hadron basis—the formation of intermediate states with different mass leads to a phase shift. It is easy to obtain an expression for the real part of the hA scattering amplitude under the same assumptions as for the expression (1):

$$\begin{aligned} \operatorname{Re} f_{\rm el}^{hA} = -4\pi\int d^2\mathbf{b}\int dM^2\left.\frac{d\sigma_{DD}^{hN}}{dM^2\,d\mathbf{q}_T^2}\right|_{q_T^2=0} \\ \times\exp\left[-\frac{1}{2}\sigma_{\rm tot}^{hN}T(\mathbf{b})\right]\int_{-\infty}^{\infty} dl_1\int_{-\infty}^{\infty} dl_2\rho(\mathbf{b},\,l_1)\,\rho(\mathbf{b},\,l_2) \\ \times\sin[q_L(l_2-l_1)]\exp[iq_L(l_2-l_1)]. \end{aligned} \tag{15}$$

Results of numerical calculations can be found in Ref. 23.

2. EFFECTS OF COLOR SCREENING

Study of the peripheral interaction of hadrons at high energies comes up against the unresolved large-distance problem of QCD. Nevertheless, one can formulate some general consequences of the fact that the interaction in QCD is a color interaction. The hadrons consist of colored objects but are themselves colorless. Their interaction resembles the interaction of neutral systems (positronium[24] atoms...) in QED. Within the hadrons the color is spatially distributed, and the interaction is of the dipole kind. One must therefore expect that if the transverse dimension of the hadron tends to zero, $\tau \to 0$, then the interaction cross section will behave as $\sigma(\tau) \propto \tau^2$. The simplest expression for $\sigma(\tau)$ that has this behavior is

$$\sigma(\tau) = \frac{\tau^2}{\langle\tau^2\rangle}\sigma_{\rm tot}. \tag{16}$$

Here, $\langle\tau^2\rangle| = \int\Psi(\boldsymbol{\tau})|^2\boldsymbol{\tau}^2 d^2\boldsymbol{\tau}$, where $\Psi(\boldsymbol{\tau})$ is the hadron wave function.

Since the work of Low[25] and Nussinov,[26] elastic scattering of hadrons has often been described[1,27] in the two-gluon approximation. The corresponding graphs are shown in Figs. 2a and 2b for meson–nucleon scattering. Summation over all ways in which the gluons can be joined to the quarks of the nucleon is understood. Naturally, the validity of the Born approximation cannot be justified in the spirit of perturbation theory, since here the coupling constant is large, $\alpha_s \approx 1$. The reason why the two-gluon approximation corresponds well to the experimental data on the total cross sections is that it correctly reproduces the dependence of the interaction cross section on the hadron size. Indeed, the contribution to $\sigma(\tau)$ of the sum of the graphs in Figs. 2a and 2b has the form

$$\sigma(\tau) = \frac{32}{3}\pi\alpha_s\int\frac{d^2\mathbf{k}}{(2\pi)^2\,\mathbf{k}^4}(1-e^{i\mathbf{k}\boldsymbol{\tau}})(1-f_N(\mathbf{k}^2)). \tag{17}$$

We choose the two-quark form factor of the nucleon in Gaussian form: $f_N(\mathbf{k}^2) \equiv \langle\exp[i\mathbf{k}(\boldsymbol{\rho}_1 - \boldsymbol{\rho}_2)]\rangle_N \exp(-\mathbf{k}^2/\lambda^2)$, where $\lambda \approx 3.2\ \mathrm{F}^{-2}$. Here, ρ_i $(i = 1, 2, 3)$ are the impact parameters of the quarks in the nucleon, with respect to

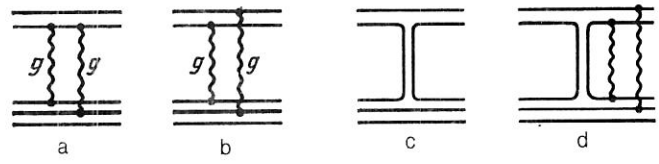

FIG. 2. Graphs describing elastic scattering (a, b) and charge exchange (c, d).

which averaging is done. The expression (17) can be reduced to the form[29]

$$\sigma(\tau)=\frac{16\pi\alpha_s^2}{3\lambda^2\ln 2}[1+C-e^{-\gamma}+\ln\gamma-(1+\gamma)\,\mathrm{Ei}(-\gamma)], \quad (18)$$

where $\gamma=\lambda^2\tau^2/4$. The constant α_s is fixed by the condition

$$\sigma_{\mathrm{tot}}^{\pi N}=(16/3)\,\pi\alpha_s^2/\lambda^2.$$

It can be seen from (18) that in the limit $\tau\to 0$ the cross section does indeed decrease as $\tau^2\ln\tau$. The factor $\ln\tau$ that is additional compared with the expression (16) is due to the contribution of the long-range dipole interaction in (17).

The smallness of the cross section for the interaction of small-radius hadrons consisting of heavy quarks is indeed confirmed experimentally. However, this is not a serious argument in support of color dynamics, since the heavier constituent quarks could have a different interaction cross section, as indeed is assumed in the constituent-quark model. It will be shown below that unique information about the behavior of $\sigma(\tau)$ can be obtained by using nuclear targets.

2.1. Absorption of hadrons by the nuclear medium

We consider the problem of absorption of high-energy hadrons on passage through a nucleus. As we have shown, the cross section for the hadron–hadron interaction depends on the transverse dimension τ of the incident hadron. Therefore, configurations with given transverse dimension τ can be taken as the interaction eigenstates. The weight coefficient for the averaging over τ is the square of the hadron wave function: $|\psi(\tau)|^2$. If the hadron energy E is sufficiently high, $E\gg\mu^2R_A$, then the quarks of the incident hadron can be regarded as "frozen" during the time of the passage through the nucleus. Therefore, the probability that the hadron passes through the nucleus without interaction is

$$W(T)=\int d^2\tau\,|\,\Psi_h(\tau)\,|^2\,e^{-\sigma(\tau)T}\equiv\langle\exp[-\sigma_a^n(\tau)\,T]\rangle. \quad (19)$$

If $\sigma(\tau)$ is substituted in (19) in the form (16), and the hadron wave function $\Psi_h(\tau)$ is taken in the Gaussian form, then

$$W(T)=(1+\sigma_{\mathrm{tot}}^{hN}\,T)^{-1}. \quad (20)$$

Thus, in place of exponential damping of the beam in the nuclear medium there is only a power-law decrease.[28–30]

This significant increase in the nuclear transparency nevertheless leads to small ($\sim 10\%$) inelastic corrections to the total cross section for the hadron–nucleus interaction even for heavy nuclei. Indeed, the greatest difference from the Glauber–Sitenko approximation can be expected in the region $\sigma_{\mathrm{tot}}^{hN}T\gg 1$, where, however, the relative contribution of the second term in (9) is small.

Knowing the elastic scattering amplitude, we can readily calculate the cross section for coherent diffraction dissociation of the hadron on the nucleus, summed over the final states:[28]

$$\sigma_{\mathrm{DD}}^{hA}=\int d^2\mathbf{b}\,[\langle f_{\mathrm{el}}^2(\mathbf{b},\tau)\rangle-\langle f_{\mathrm{el}}(\mathbf{b},\tau)\rangle^2]. \quad (21)$$

Here, $f_{\mathrm{el}}(\mathbf{b},\tau)=1-\exp[-1/2\sigma(\tau)T(\mathbf{b})]$.

The expression (21) does not contain unknown parameters, and the results of the calculation[29] correspond well to the experimental data.

The process of coherent diffraction dissociation on nuclei has been used for many years as a way of obtaining information about the interaction cross section of the unstable hadrons produced in this process; as a rule, this cross section has been found to be anomalously small. That there is an error here can be demonstrated by the following "theoretical experimental."[31] We calculate the cross section for coherent diffraction dissociation of a pion on a nucleus in accordance with the expression (21) and compare the result with the corresponding expression in the Glauber–Sitenko approximation.[32] The result σ_x found in this manner decreases with increasing atomic number of the nucleus and even becomes less than $\sigma_{\mathrm{tot}}^{\pi N}$. However, it is clear that the smallness of σ_x is a consequence of neglect of the inelastic corrections, which appreciably increase the cross section. The parameter σ_x is not the cross section for the interaction of the produced hadrons, since at high energies they are formed outside the nucleus.

2.2. Coherent regeneration of K_S mesons on nuclei

Processes in which the wave that has passed through the nucleus is detected are the most suitable for testing the relations (16) and (18). An example of this is the coherent regeneration of K_S mesons on nuclei.[33] This process is also remarkable in that the exchange of the ω Reggeon responsible for the CP charge exchange $K_L\to K_S$ selects in the incident K_L beam fluctuations with increased size:

$$R^2(E)=R_0^2+4\alpha'_\omega\ \ln(s/s_0). \quad (22)$$

Here, $\alpha'_\omega\approx 0.75\ (\mathrm{GeV}/c)^{-2}$ is the slope parameters of the ω trajectory, and $R_0^2\sim 0.26\ \mathrm{F}^2$ is the mean-square radius of the K meson. Because of the large value of α'_ω, the value of $R^2(E)$ increases rapidly with the energy and considerably exceeds R_0^2. One can therefore expect enhanced absorption of K mesons by a nucleus. The amplitude of coherent regeneration of K_S mesons on nuclei has the form

$$f_{LS}^A=f_{LS}^N\int d^2\mathbf{b}T(\mathbf{b})\left\langle\exp\left[-\frac{1}{2}\sigma(\tau)\,T(\mathbf{b})\right]\right\rangle. \quad (23)$$

In the averaging over τ in (23) allowance has been made for the increase with the energy of the interaction range (22).

The results of the calculation are compared with the

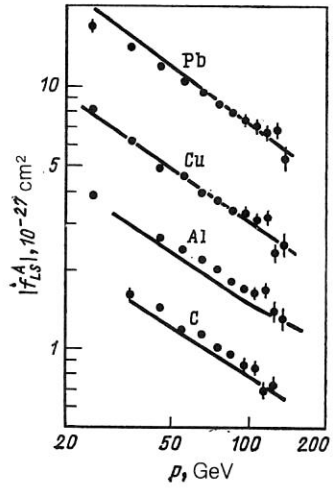

FIG. 3. Amplitude of coherent regeneration $K_L\to K_S$ on various nuclei. The curves are calculated with the cross section $\sigma(\tau)$ obtained in the two-gluon approximation. The data are from Ref. 34.

data of Ref. 34 in Fig. 3. The calculation matches the data well. Note that allowance for the inelastic corrections in accordance with Eq. (1) has led to an appreciable divergence from the data of Ref. 34.

Since these calculations do not contain free parameters, the results are an important confirmation of the correctness of the approach. Nevertheless, the comparison cannot be regarded as critical, since an analogous calculation in the constituent-quark model[35] also led to good agreement.

2.3. Quasielastic scattering of hadrons by nuclei

We shall discuss the possibility of testing the predictions of QCD in quasielastic scattering of hadrons by nuclei. It may be expected that in hadron–nucleus scattering with momentum transfer q the form factor "selects" in the hadron fluctuations with small transverse dimension $\tau \sim 1/q$. Therefore, if the scattering occurs in the presence of a nuclear medium, the absorption of the hadron in accordance with (16) will depend strongly on q and must vanish with increasing q. The value of $A_{\text{eff}}(\mathbf{q}^2) = (d\sigma^{hA}/d\mathbf{q}^2)/d\sigma^{hN}/d\mathbf{q}^2)$ must increase sharply from $A^{1/3}$ when $\mathbf{q}^2 \ll (\tau^2)^{-1}$ to $\sim A$ when $\mathbf{q}^2 \gg (\tau^2)^{-1}$.

The cross section of single quasielastic scattering by a nucleus can be expressed in the form[36,37]

$$\frac{d\sigma^{(1)}_{Q\,\text{el}}}{d\mathbf{q}^2} = \frac{1}{4\pi}\int d^2\mathbf{b}T(\mathbf{b})\left|\left\langle f_{\text{el}}(\mathbf{q},\tau) \times \exp\left[-\frac{1}{2}\sigma(\tau)T(\mathbf{b})\right]\right\rangle\right|^2 \quad (24)$$

We calculate the amplitude for elastic meson–nucleon scattering, $f_{\text{el}}(\mathbf{q},\tau)$, and the total cross section in the two-gluon approximation.

The results of the calculation of $A^{(1)}_{\text{eff}}(\mathbf{q}^2)$ for a number of nuclei, made in accordance with Eq. (24), are shown by the broken curves in Fig. 4. The dotted lines show the calculation in the Glauber–Sitenko approximation. It can be seen that $A_{\text{eff}}(\mathbf{q}^2)$ increases much slower than expected. The effect is of the same order as in the constituent-quark model.[38] It is readily seen that the reason for this is that when $\mathbf{q}^2 \gtrsim (\tau^2)^{-1}$ the elastic scattering is dominated by the graph in Fig. 2b, which does not contain the meson form factor and does not distinguish small sizes.

It can also be seen from Fig. 4 that at small $\mathbf{q}^2$ the Glauber–Sitenko approximation overestimates the cross section, i.e., the elastic corrections in this process make the nucleus less transparent. The reasons for this, and also some consequences, will be considered in Sec. 2.6.

Note that for much larger values $\mathbf{q}^2 \gg [2\alpha'_p \ln(s/s_0)]^{-1}$ the nuclear screening in quasielastic scattering must still vanish.[39] For if the scattering of quarks with large momentum transfer is not to be accompanied by gluon bremsstrahlung, both the quarks and their color field must be localized in a small region of τ. Experimental verification requires obligatory detection of the recoil nucleon and reconstruction of the quasielastic kinematics in order to eliminate the contribution of multiple scatterings. Otherwise these must be calculated. The contribution of double scattering has the form[36,37]

$$\frac{d\sigma^{(2)}_{Q\,\text{el}}}{d\mathbf{q}^2} = \frac{1}{8\pi}\int d^2\mathbf{b}T^2(\mathbf{b})\int\frac{d^2\mathbf{k}}{(2\pi)^2} \times\left|\left\langle f_{\text{el}}(\mathbf{k},\tau) f_{\text{el}}(\mathbf{q}-\mathbf{k},\tau)\exp\left[-\frac{1}{2}\sigma(\tau)T(\mathbf{b})\right]\right\rangle\right|^2. \quad (25)$$

For small $\mathbf{q}^2 \lesssim 1$ GeV/c^2 this expression can be estimated in the Glauber–Sitenko approximation, since the inelastic corrections here are small and the momentum transfer is on the average divided equally between the two scatterings. The value of $A_{\text{eff}}(\mathbf{q}^2)$ with allowance for (25) is shown in Fig. 4 by the continuous curve. As the calculation shows, the contribution of triple scattering is negligibly small in this region of $\mathbf{q}^2$.

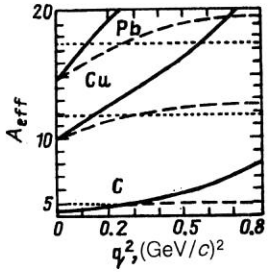

FIG. 4. Predictions for $A_{\text{eff}}(q^2)$ in quasielastic scattering. The broken curves correspond to the contribution of single scattering calculated in the two-gluon approximation; the continuous curves, to the calculation with the addition of multiple scattering; the dotted lines, to the Glauber–Sitenko approximation.

2.4. Quasifree charge exchange of hadrons on nuclei

In contrast to quasielastic scattering, in the charge-exchange reaction one can expect appreciable growth of $A_{\text{eff}}(\mathbf{q}^2)$, since the graph in Fig. 2c, corresponding to Reggeon exchange, contains the hadron form factor. Therefore, in the region of $\mathbf{q}^2$ values in which the contribution of branch cuts can be ignored, the contribution of the compressed meson configurations to the charge-exchange reaction will be enhanced.[31,37]

We first consider the reaction $\pi^- p \to \eta^0 n$ where for $\mathbf{q}^2 \lesssim 1$ GeV^2 the contribution of the pole A_2 is dominant. The cross section for single charge exchange without rescattering has the form[37]

$$\frac{d\sigma^{(1)}(\pi^- A \to \eta^0 X)}{d\mathbf{q}^2} = \frac{1}{8\pi}\frac{Z}{A}\int d^2\mathbf{b}T(\mathbf{b})\,\text{Sp}\{\langle\hat{f}^+_{\text{cex}}(\mathbf{q},\tau)\,e^{-\frac{1}{2}\sigma(\tau)T(\mathbf{b})}\rangle \times\langle\hat{f}_{\text{cex}}(\mathbf{q},\tau)\,e^{-\frac{1}{2}\sigma(\tau)T(\mathbf{b})}\rangle\}. \quad (26)$$

Here the averaging over τ is done with weight factor $\Psi_\pi(\tau)\Psi^*_\eta(\tau)$. In what follows we shall assume that the spatial parts of the π and η wave functions are the same (in accordance with SU_3), i.e., $\sigma^{\pi N}_{\text{tot}} = \sigma^{\eta N}_{\text{tot}}$.

The amplitude $f_{\text{cex}}(\mathbf{q},\tau)$ is a 2×2 matrix in the nucleon spin space. It can be expressed in the form

$$\hat{f}_{\text{cex}}(\mathbf{q},\tau) = C\,[A(\mathbf{q},\tau) + i\,|\,\mathbf{q}\,|\,(\sigma\mathbf{n})\,B(\mathbf{q},\tau)]. \quad (27)$$

Here C includes all the factors that are independent of $\mathbf{q}$ and τ; $\mathbf{n}$ is the unit vector normal to the reaction plane, and $\boldsymbol{\sigma}$ are the Pauli matrices. The amplitudes A and B can be written in the form

$$\left.\begin{aligned} A(\mathbf{q},\tau) &= \exp(i\mathbf{q}\tau/2 - \lambda\mathbf{q}^2);\\ B(\mathbf{q},\tau) &= \beta A(\mathbf{q},\tau). \end{aligned}\right\} \quad (28)$$

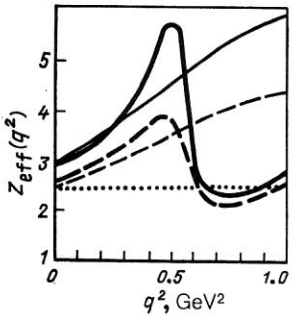

FIG. 5. $Z_{\text{eff}}^{(1)}(q^2)$ for charge exchange on the ^{12}C nucleus. The continuous and broken curves correspond to the calculation in versions 1 and 2, respectively. The thin curves relate to the $\pi^- \to \eta^0$ reaction and dominance of Regge poles in the $\pi^- \to \pi^0$ reaction; the heavy curves correspond to the charge-exchange reaction $\pi^- \to \pi^0$ with allowance for branch points; the dotted line is the calculation in the Glauber–Sitenko approximation.

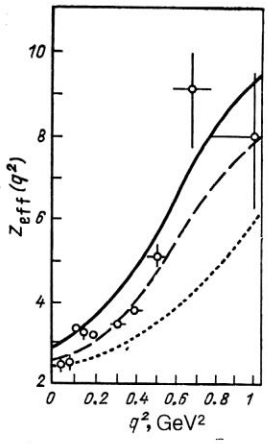

FIG. 6. $Z_{\text{eff}}(q^2)$ for the charge-exchange reaction $\pi^- C \to \eta^0 X$. The data are from Ref. 41, and the calculations were made with allowance for rescattering in version 1 (continuous curve), in version 2 (dashed curve), and in the Glauber–Sitenko approximation (dotted curve).

The fit to the experimental data[40,41] at 40 GeV gives $\beta = 6.1\ \text{GeV}^{-1}$, $\lambda = 3.4\ (\text{GeV}/c)^{-2}$.

We calculate $Z_{\text{eff}}(q^2)$ for two forms of the dependence $\sigma(\tau)$: 1) $\sigma(\tau)$ is calculated in accordance with the expression (16); 2) $\sigma(\tau)$ is calculated in the two-gluon approximation in accordance with the expression (18). The results of the calculation of $Z_{\text{eff}}^{(1)}(\mathbf{q}^2)$ in accordance with the expression (26) for the ^{12}C nucleus are given in Fig. 5 by the thin continuous and broken curves. The dotted line shows the result of the Glauber–Sitenko approximation. It can be seen that $Z_{\text{eff}}^{(1)}(\mathbf{q}^2)$ does indeed increase with $\mathbf{q}^2$ much faster than in quasielastic scattering.

If the recoil nucleon is not detected, it is necessary to take into account multiple scattering. The contribution of charge exchange with additional elastic rescattering has the form

$$\frac{d\sigma^{(2)}(\pi^- A \to \eta^0 X)}{d\mathbf{q}^2} = \frac{1}{8\pi}\frac{Z(A-1)}{A^2}\int d^2\mathbf{b}\,T^2(\mathbf{b}) \times \int \frac{d^2\mathbf{k}}{(2\pi)^2}\,\text{Sp}\,\{\langle \hat{f}_{\text{cex}}^{+}(\mathbf{k},\tau)\,\hat{f}_{\text{el}}^{*}(\mathbf{q}-\mathbf{k},\tau)\,e^{-\frac{1}{2}\sigma(\tau)T(\mathbf{b})}\rangle \times \langle \hat{f}_{\text{cex}}(\mathbf{k},\tau)\,f_{\text{el}}(\mathbf{q}-\mathbf{k},\tau)\,e^{-\frac{1}{2}\sigma(\tau)T(\mathbf{b})}\rangle\}. \quad (29)$$

This expression, like (25), can be estimated in the Glauber–Sitenko approximation, and the rescatterings of higher order can be ignored. The result of the summation of (26) and (29) is compared in Fig. 6 with the data of Ref. 41. It can be seen that there is good agreement. At the same time the Glauber–Sitenko approximation significantly underestimates the cross section.

A specific feature of the $\pi^- p \to \pi^0 n$ reaction is the minimum in the differential cross section at $q^2 \approx 0.6\ \text{GeV}^2$. Two explanations of this phenomenon are known. One[42] attributes the minimum to the vanishing of the residue of the ρ pole at a point with "incorrect" signature. The other possible reason is destructive interference of the contribution of the ρ pole and the ρ–P branch point in the spin-flip amplitude.[42] Both interpretations have difficulties, and it is not yet known which is correct.

Study of the quasifree charge exchange $\pi^- \to \pi^0$ on nuclei opens up new possibilities for discriminating mechanisms of charge exchange on nucleons. In the first case, the behavior of $Z_{\text{eff}}(\mathbf{q}^2)$ hardly differs from the calculations for the reaction $\pi^- p \to \eta^0 n$, which are shown in Fig. 5. In the second case, the interference of the pole and the branch point on the nucleus takes place in a different way than on hydrogen. Indeed, in the region of the minimum the pole graph shown in Fig. 2c is enhanced on the nucleus by a factor $Z_{\text{eff}}^{\text{pole}} \approx Z$. In the graph in Fig. 2c, corresponding to the ρ–P branch point, momentum is transferred to both quarks of the meson, there is no form factor, and this contribution is enhanced on the nucleus only by a factor $Z_{\text{eff}}^{\text{cut}} \approx Z^{1/3}$. Therefore, the minimum in the cross section of single charge exchange on a nucleus must be shifted to larger values of $\mathbf{q}^2$, and must disappear entirely on heavy nuclei.[31,36] The spin amplitudes of $\pi^- p \to \pi^0 n$ charge exchange differ from (28) when allowance is made for the branch points and have the form

$$\left.\begin{aligned} A(\mathbf{q},\tau) &= \exp(i\mathbf{q}\tau/2 - \lambda\mathbf{q}^2) - \gamma/2a\,\exp(-a\mathbf{q}^2/2 - \tau^2/8a);\\ B(\mathbf{q},\tau) &= \beta\exp(i\mathbf{q}\tau/2 - \lambda\mathbf{q}^2) - \beta\gamma/4a\,\exp(-a\mathbf{q}^2/2 - \tau^2/8a).\end{aligned}\right\} \quad (30)$$

The parameters $\gamma, \beta, \lambda, a$ were found from a comparison with the data of Refs. 40 and 41: $\gamma = 5.95\ \text{GeV}^{-2}$, $|\beta| = 3.7\ \text{GeV}^{-1}$, $\lambda = 4.5\ \text{GeV}^{-2}$, $a = 6\ \text{GeV}^{-2}$.

The results of the calculation of $Z_{\text{eff}}^{(1)}(\mathbf{q}^2)$ are shown in Fig. 5 by the heavy continuous and dashed curves. The complicated shape of the curves is explained by the displacement of the position of the minimum in the cross section for charge exchange on the nucleus as compared with a hydrogen target. It can be seen that the $\mathbf{q}^2$ dependence of $Z_{\text{eff}}^{(1)}(\mathbf{q}^2)$ is essentially determined by the part played by the branch points in the $\pi^- p \to \pi^0 n$ reaction.

Unfortunately, the existing data[41] do not distinguish the contribution of single charge exchange, and it is therefore necessary to take into account the correction for the additional rescattering, calculated in accordance with (29), in which $\hat{f}_{\text{cex}}$ is given by the expressions (27) and (30).

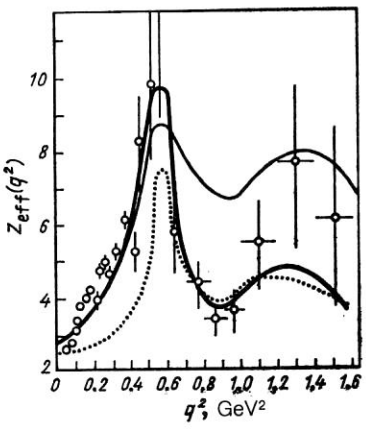

FIG. 7. The same as in Fig. 6 but for the reaction $\pi^- A \to \pi^0 A'$. The heavy and thin curves were obtained in version 1 with and without allowance for the contribution of branch points; the dotted curve is the calculation in the Glauber–Sitenko approximation.

The results of the calculation are compared with the data of Ref. 41 in Fig. 7. It can be seen that the Glauber–Sitenko approximation is in strong disagreement with the data and that calculation in version 1 with amplitude $\hat{f}_{cex}$ containing a contribution of the branch points agrees better than the other versions.

Note that in the constituent-quark model Z_{eff} depends on $\mathbf{q}^2$ in the same way as in quasielastic scattering,[38] i.e., much more weakly than in the experiment. This also applies to the version of the model of Ref. 43.

In Ref. 44 data were obtained for the charge-exchange reaction $\pi^+ C \to K^+ YX$. An accurate measurement of the missing mass suppressed the contribution of multiple scattering. Thus, the data shown in Fig. 8 relate to $A_{\text{eff}}^{(1)}$. Comparison with the calculations in version 1 confirms the QCD prediction. It is important that the effect here is a qualitative one.

Thus, the data on quasifree charge exchange on nuclei have a high sensitivity to the behavior of $\sigma(\tau)$. They are also interesting in that allowance for the inelastic corrections changes the cross section by several times.

2.5. Polarization in quasielastic scattering

Polarization in elastic scattering at high energies is due to interference of the Pomeron amplitude with the Reggeon amplitude, which is small. As was shown, in single quasielastic scattering at $\mathbf{q}^2 \gg \langle \tau^2 \rangle^{-1}$ the Reggeon amplitude is not screened and is enhanced by a factor A. At the same time, the Pomeron contribution is enhanced by only a factor $A^{1/3}$. Thus, the ratio of the amplitudes with and without spin flip on the nucleus is changed, and the polarization must increase.[31,36,37]

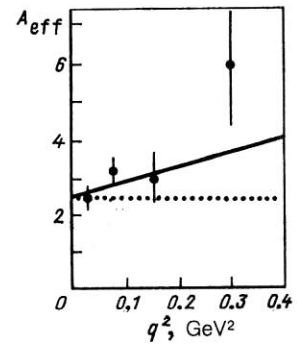

FIG. 8. $A_{\text{eff}}(q^2)$ for the reaction $\pi^+ C \to K^+ YX$. The continuous line is the calculation in version 1, and the dotted line corresponds to the Glauber–Sitenko approximation.

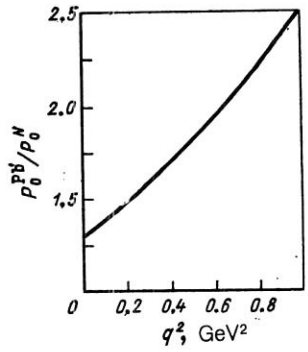

FIG. 9. Prediction for the ratio of the polarizations in quasielastic scattering on Pb and on the nucleon.

The polarization parameter $P_0^A(q^2)$ can be calculated in accordance with the formula

$$P_0^A(\mathbf{q}^2)\frac{d\sigma_{Q\,\text{el}}^{hA}}{d\mathbf{q}^2} = \frac{Z}{4\pi A}\int d^2\mathbf{b}\,T(\mathbf{b}) \times \text{Sp}\{(\sigma\mathbf{n})\langle \hat{f}_{\text{el}}^{+}(\mathbf{q},\tau)\, e^{-\frac{1}{2}\sigma(\tau)T(\mathbf{b})}\rangle \langle \hat{f}_{\text{el}}(\mathbf{q},\tau)\, e^{-\frac{1}{2}\sigma(\tau)T(\mathbf{b})}\rangle\}. \quad (31)$$

The cross section $d\sigma_{Q\,\text{el}}^{hA}/d\mathbf{q}^2$ is given by the expression (26). The scattering amplitude is the sum of the Pomeron and Reggeon contributions: $\hat{f}_{\text{el}}(\mathbf{q},\tau) = \hat{f}_{\text{el}}^{P}(\mathbf{q},\tau) + \hat{f}_{\text{el}}^{R}(\mathbf{q},\tau)$. The amplitudes $\hat{f}_{\text{el}}^{P,R}$ have the form (27). We set $B^P(\mathbf{q},\tau) = 0$ and take $B^{Pp}(\mathbf{q},\tau)$ in the form (30), i.e., we take into account the contribution of the branch points.

The results of a calculation[37] for the ratio of the polarization of the recoil protons in quasielastic scattering by the ^{208}Pb nucleus to the polarization in elastic πp scattering are shown in Fig. 9. It can be seen that for $\mathbf{q}^2 \approx 1$ GeV^2 the nuclear enhancement factor exceeds 2.

Note than an effect of the same order is expected for a beam of protons quasielastically scattered by a nuclear target.

2.6. Inclusive production of hadrons on nuclei in the three-Reggeon region

We consider the inclusive charge exchange $a + b \to c + X$ in the three-Reggeon region of the kinematic variables: $s/M_x^2 \gg 1$, $M_x^2 \gg 1$ GeV^2. In the cross section of this process we can distinguish contributions of three-Reggeon graphs of two types: RRR and RRP, which are shown in Figs. 10 and 11. The broken line denotes the operation of taking the absorption part. The dependence of the contributions of these graphs on the Feynman variable x_F is given by the expressions[45]

$$\left(\frac{d^2\sigma}{dx_F\, d\mathbf{q}^2}\right)_{RRR} = \frac{1}{\sqrt{s/s_0}}\frac{G_{RRR}(0)}{\sqrt{1-x_F}} \times \exp\{-\mathbf{q}^2[R_{RRR}^2 - 2\alpha_R' \ln(1-x_F)]\}; \quad (32)$$

$$\left(\frac{d^2\sigma}{dx_F\, d\mathbf{q}^2}\right)_{RRP} = G_{RRP}(0) \times \exp\{-\mathbf{q}^2[R_{RRP}^2 - 2\alpha_R' \ln(1-x_F)]\}. \quad (33)$$

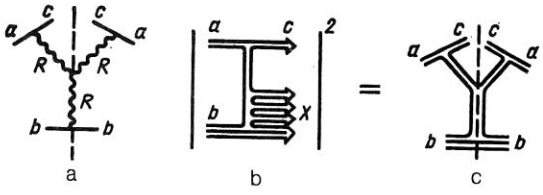

FIG. 10. Structure of the three-Reggeon RRR graph.

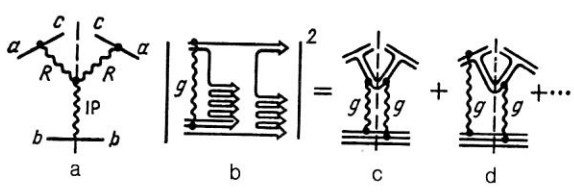

FIG. 11. Structure of the three-Reggeon RRP graph.

Here, $G(\mathbf{q}^2) = G(0)\exp(-\mathbf{q}^2R^2)$ are the corresponding effective three-Reggeon vertices.

The diagrams in Fig. 10a correspond to the planar graphs shown in Figs. 10b and 10c. The process occurs as follows.

The quarks of the incident hadron are in a configuration that is strongly asymmetric with respect to the momenta—one of the quarks carries all the momentum. The probability of such a configuration is suppressed by the factor $1/\sqrt{s}$. After the slow quark (antiquark) has been annihilated, fragmentation of the fast quark begins, for example, by breaking of the color triplet string formed between a fast quark and a target diquark (to be definite, suppose $b \equiv N$). The fragmentation takes place only up to momenta $p \approx (1-x_F)s/(2m_N)$, after which an antiquark with this momentum is immediately captured by the leading quark. The probability of such capture is $dx_F/\sqrt{1-x_F}$. All these factors are indeed contained in the expression (32).

The interpretation of the RRP graph in Fig. 11a is less trivial. The incident meson, as shown in Fig. 11b, is in a configuration in which the fast quark carries the momentum fraction x_1, and the slow quark carries the fraction $1-x_1$. The probability of this is $1/\sqrt{1-x_1}$. After the exchange of a gluon between one of the quarks and the target the slow quark completely fragments into a jet with mass $M_1 = \sqrt{s(1-x_1)}$, while the fast quark fragments to mass $M_2 = \sqrt{s(1-x_F)/x_1}$ and then captures a quark with momentum $p \approx (1-x_F/x_1)s/2m_N$. The probability of such capture is $1/\sqrt{1-x_F/x_1}$. The product of the structure function of the incident meson and the fragmentation function must be integrated over x_1, and this gives

$$\int dx_1 dx_2\, \delta(x_1x_2 - x_F)\, \frac{1}{\sqrt{1-x_1}\sqrt{1-x_2}} = \int_{x_F}^{1} dx_1\, \frac{1}{\sqrt{x_1(1-x_1)(x_1-x_F)}}. \tag{34}$$

It is easy to see that for $1-x_F \ll 1$ this integral does not depend on x_F. Now this corresponds to the expression (33) and is a consequence of the nonplanar (cylindrical) shape of the graph in Fig. 11.

Although the quark diagrams in Figs. 11b and 11c lead to an x_F dependence corresponding to the three-Reggeon phenomenology (33), there is nevertheless a fundamental difference between the graphs in Fig. 11a and Figs. 11c and 11d. The usual interpretation of the graph in Fig. 11a is that the Reggeon R is elastically scattered by the target through Pomeron exchange. However, it can be seen that the graph in Fig. 11c does not have an analogous graph that screens the color in the Reggeon (cf. Figs. 2a and 2b). Moreover, the graph in Fig. 11d does not admit a three-Reggeon interpretation at all. The reason for this lack of correspondence is that in QCD perturbation theory the concept of a three-Reggeon vertex localized in the rapidity scale is meaningful only for the vertex RRR, as in Fig. 10. In contrast to the scalar $\lambda\varphi^3$ theory, which was usually used earlier to interpret Reggeon graphs, in QCD an interaction with a large rapidity interval through gluon exchange is possible. Therefore, the use of the graphs RRP, PPP, etc., is possible only for purposes of phenomenology, since they give the correct x_F dependence.

We consider the question of the nuclear enhancement of three-Reggeon graphs.[46] Since the slope parameters that determine the $\mathbf{q}^2$ dependence of the cross section on nuclear and hydrogen targets differ little,[44] for estimates we restrict ourselves to a calculation of A_{eff} for $\mathbf{q}^2 = 0$, when the calculations are much simpler. Since the Reggeon amplitude (27) at $\mathbf{q}^2 = 0$ does not depend on τ, the expression (26) in the version (16) reduces to the form

$$A_{\text{eff}}^{R} = \int \frac{d^2\mathbf{b}T(\mathbf{b})}{\left[1+\frac{1}{2}\sigma_{\text{tot}}^{hN}T(\mathbf{b})\right]^2}. \tag{35}$$

On the other hand, in the RRP graph the colors of the quarks of the incident hadron are mutually screened, as can be seen in Figs. 11c and 11d. For this reason, the amplitude of the reaction on the nucleon at $\mathbf{q}^2 = 0$ is proportional to τ^2, i.e., the result for A_{eff}^{P} must be the same as in quasielastic scattering:

$$A_{\text{eff}}^{P} = \int \frac{d^2bT(b)}{\left[1+\frac{1}{2}\sigma_{\text{tot}}^{hN}T(b)\right]^4}. \tag{36}$$

Although the T dependence of the integrands in (35) and (36) is a power law and asymptotically weaker than

TABLE I. Effective nuclear numbers calculated in the Glauber–Sitenko approximation, and also for the RRP and RRR graphs.

Target nucleus	$A_{\text{eff}}^{\text{GSA}}$	A_{eff}^{P}	A_{eff}^{R}
Be	4.9	3.5	5.4
Al	9.1	5.8	11.4
Cu	15.0	9.0	21.1
Pb	23.4	13.2	44.0

exponential, nevertheless for real nuclei, as can be seen from Table I,

$$A_{\text{eff}}^{R} > A_{\text{eff}}^{\text{GSA}}, \quad \text{but } A_{\text{eff}}^{P} < A_{\text{eff}}^{\text{GSA}}.$$

(Here, GSA denotes the Glauber–Sitenko approximation.)

In other words, the inelastic corrections, as we have already said, can "lighten" but they can also "darken" the nucleus. This depends on the process.

Now in accordance with (32) and (33) the *RRR* and *RRP* graphs are associated with different dependences on x_E, and their contributions to the cross section for the reaction on the nuclear target are enhanced differently, so that we must expect a nontrivial x_F dependence of $A_{\text{eff}}(x_F)$. The contribution of the *RRR* graph decreases with the energy as $1/\sqrt{s}$, and therefore we take the data of Ref. 47 for the $\pi^+ A \to \eta^0 X$ reaction at 10.5 Gev. It is true that at such a low energy and $x_F \approx 1$ it is necessary to introduce nonasymptotic corrections to the expression (33), which does not take into account the relative phase space of the two jets (see Fig. 11b). In the limit $x_F \to 1$ each jet goes over into a resonance, and near the threshold $M_0 = m_1 + m_2$ for the production of two hadrons we obtain a suppression factor Ω due to the two-particle phase space:

$$\Omega = \sqrt{M_X^2 - (m_1 + m_2)^2}/M_X. \tag{37}$$

This factor has an effect only when $1 - x_F \approx (m_1 + m_2)^2/s$, i.e., at high energies it can be omitted.

The minimal masses that can be substituted in (37) are $m_1 = m_\pi$, $m_2 = m_N$. However, the probability of recombination of quarks into a pion is suppressed by a factor 1/3 compared with the ρ meson. Comparison of the data on the cross sections of the reactions $\pi^- p \to \eta n$ and $\pi^+ p \to \eta \Delta^{++}(1236)$ shows that the isotopic amplitudes of these processes with $I = 3/2$ and $I = 1/2$ are approximately equal. This means that for the interaction with the deuteron (and with heavy nuclei) a target diquark fragments into $\Delta(1236)$ with a probability two times greater than into a nucleon.

Thus, we take as an estimate in the factor (37) the values $m_1 = m_\rho$, $m_2 = m_\Delta$.

Ignoring the corrections for rescattering in the deuteron, we write down for the ratio $R_{A/d}(x_F) = d\sigma/dx_F(\pi^+ A \to \eta^0 X)/d\sigma/dx_F(\pi^+ d \to \eta^0 X)$ the expression

$$R_{A/d}(x_F) = \frac{1}{2}\left(\frac{A_{\text{eff}}^{R}/\sqrt{s/s_0} + \lambda A_{\text{eff}}^{P}\sqrt{x_0 - x_F}}{1/\sqrt{s/s_0} + \lambda\sqrt{x_0 - x_F}}\right). \tag{38}$$

We have here used the expressions (32) and (33), in which it is assumed that $R_{RRR}^2 = R_{RRP}^2$ and $\lambda = G_{RRP}(0)/G_{RRR}(0) \approx 1$, this corresponding well to the data on binary reactions; to (33) the factor (37) has been added; $x_0 = 1 - (m_\rho + m_\Delta)^2/s$; for $x > x_0$ the contribution of the *RRP* graph is equal to zero; it is assumed that the dependence of the cross section on $\mathbf{q}^2$ is the same for all nuclei.

The results of the calculation are compared with the data of Ref. 47 for the ^{64}Cu nucleus in Fig. 12.

Naturally, with increasing energy the relationship between the *RRP* and *RRR* graphs changes, as can be seen from (32) and (33). The region in which the *RRR* graph is dominant is shifted to the region of large $x_F \to 1$. In addition, the fragmentation-length effects become noticeable (see Sec. 4.4), leading to a growth of A_{eff} with increasing $1 - x_F$. The corresponding predictions for $R_{Cu/d}$ at energy 40 GeV are shown in Fig. 12.

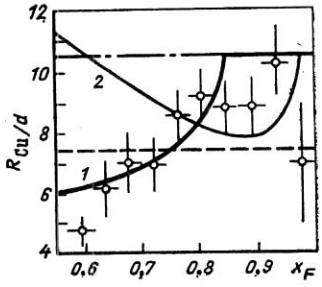

FIG. 12. Data on Ref. 47 for the ratio $R_{Cu/d}$. The broken line corresponds to the calculation in the Glauber–Sitenko approximation; 1) calculation in accordance with the expression (38); 2) the prediction for energy 40 GeV with allowance for the hadronization time of the quarks; the chain line is the calculation for $\frac{1}{2}A_{\text{eff}}^{R}$.

3. MULTIPLE COLOR CHARGE EXCHANGES IN HADRON–NUCLEUS INTERACTIONS

A widely held view of the mechanism of inelastic interaction of hadrons at high energies is that the hadrons exchange color (in the simplest case, a gluon), and then the colored objects, separating with a large relative momentum, fragment into hadrons, the hadronization taking a long time $\sim\sqrt{s}$ (in the center-of-mass system). It follows from this that the contribution of Pomeron exchange to the elastic amplitude has a color structure (in the simplest case, it is a two-gluon exchange). When a hadron interacts with a nucleus, the Pomeron can "split" i.e., there can be double color charge exchange on two nucleons. One can also consider the case of multiple color charge exchanges of a hadron on the nucleons of a nucleus.

3.1. Validity of the Glauber–Sitenko approximation when allowance is made for the color structure of the Pomeron

The picture described above should be tested in the first place by considering the corrections[48,49] to the cross section for elastic hadron–nucleus scattering calculated in the Glauber–Sitenko approximation (with allowance for the inelastic corrections). These corrections must be small, since the standard scheme[2)] describes the data on the total cross sections for *pd* scattering with good accuracy. Therefore, the correction $\Delta_Q\sigma_{\text{tot}}$ to the total cross section that we are discussing here cannot be large:[51]

$$\Delta_Q\sigma_{\text{tot}}(pd) \lesssim 0.4 \cdot 10^{-27}\text{cm}^2. \tag{39}$$

This condition must yield certain bounds on the six-quark component of the deuteron wave function. This can be expressed by means of the resonating-group method in the form (with allowance for one *NN* channel)

$$\Psi_{NN}(1, \ldots, 6) = A_{NN}^{-1}\left(1 - \sum_{\alpha=1}^{3}\sum_{\beta=4}^{6}\hat{P}_{\alpha\beta}\right)\Psi_N(1, 2, 3)\,\Psi_N(4, 5, 6)\,F(R). \tag{40}$$

Here, $P_{\alpha\beta}$ is the operator of quark interchange, Ψ_N is the quark wave function of the nucleon, and A_{NN} is a normalization factor.

A wave function of more general form may, in addition,

include an admixture of an excited state like a six-quark bag, $\Psi_{S^6}(1,\ldots,6)$, to which we shall ascribe the S^6 configuration:

$$\Psi_d(1,\ldots,6)=\alpha\Psi_{NN}(1,\ldots,6)+\beta\Psi_{S6}(1,\ldots,6); \quad (41)$$
$$\alpha^2+2\alpha\beta\langle\Psi_{S6}\mid\Psi_{NN}\rangle+\beta^2=1.$$

We express the spatial part of the wave function of the nucleon and the $6q$ bag in the form specified by the oscillator model:

$$\Phi_n(\mathbf{r}_1,\ldots,\mathbf{r}_n)=A_n^{-1}\exp\Big[-\frac{1}{2nR_n^2}\sum_{i>j}(\mathbf{r}_i-\mathbf{r}_j)^2\Big]; \quad (42)$$
$$A_n=(\pi R_n^2)^{\frac{3}{4}(A-1)}n^{3/4},$$

where n is the number of quarks. For the nucleon radius we use the value $R_N=R_3=0.8$ F, and we shall regard R_6, the radius of the S^6 state, as a free parameter.

For the S^6 configuration there exists only one $6q$ state with the quantum numbers of the deuteron.[52] Its wave function in the STC space (spin, isospin, color) can be written in the form

$$\Psi_{S^6}^{STC}(1,\ldots,6)=A_6^{STC}\Big(1-\sum_{\alpha=1}^{3}\sum_{\beta=4}^{6}P_{\alpha\beta}\Big)\Psi_N^{STC}(1,2,3)$$
$$\times\Psi_N^{STC}(4,5,6)F_d^{ST}; \quad (43)$$
$$A_6^{STC}=10/3,$$

where ψ_N^{STC} is the nucleon wave function in the STC space, and F_d^{ST} is the nucleon wave function of the deuteron in the ST space. We calculate the correction that we seek to the total cross section, $\Delta_Q\sigma_{\text{tot}}^{pd}$, in accordance with the formula

$$\Delta_Q\sigma_{\text{tot}}(pd)=\sigma_{\text{tot}}^{2g}(pd)-2\sigma_{\text{tot}}^{2g}(pN), \quad (44)$$

where σ_{tot}^{2g} is the cross section calculated in the two-gluon approximation.

The amplitude for elastic scattering of hadrons h_1 and h_2 that consist, respectively, of n_1 and n_2 quarks described by nonrelativistic wave functions has the form

$$T_{h_1h_2}^{2g}(\mathbf{q})=\frac{18\alpha_s n_1n_2}{9}\int d^2\mathbf{k}\,\frac{V_1(\mathbf{q},\mathbf{k})V_2(\mathbf{q},\mathbf{k})}{\Big[\Big(\frac{\mathbf{q}}{2}+\mathbf{k}\Big)^2+m_g^2\Big]\Big[\Big(\frac{\mathbf{q}}{2}-\mathbf{k}\Big)^2+m_g^2\Big]}. \quad (45)$$

We have here used the notation

$$V_j(\mathbf{q},\mathbf{k})=F_j(\mathbf{q})-G_j(\mathbf{q},\mathbf{k}), \quad (46)$$

where $F_j(\mathbf{q})=\langle\Psi_j|e^{i\mathbf{qk}}|\Psi_j\rangle$, $G_j(\mathbf{q},\mathbf{k})=\langle\Psi_j|\hat{\Lambda}_j(\mathbf{q},\mathbf{k})|\Psi_j\rangle$, with

$$\hat{\Lambda}_j(\mathbf{q},\mathbf{k})=\frac{3}{16}(1-n_j)\lambda_1^\alpha\lambda_2^\alpha$$
$$\times\exp\Big[i\Big(\frac{\mathbf{q}}{2}+\mathbf{k}\Big)\mathbf{r}_1+i\Big(\frac{\mathbf{q}}{2}-\mathbf{k}\Big)\mathbf{r}_2\Big]. \quad (47)$$

We calculate the correction $\Delta_Q\sigma_{\text{tot}}(pd)$ to the total cross section in accordance with the expressions (44)–(46) with the deuteron wave function (40). We take the spatial part of the function $F(R)$ [denoting it by $f(R)$], which describes the relative motion of the clusters in the wave function (40), in the form corresponding to the Reid potential with a soft core. We obtain $\Delta_Q\sigma_{\text{tot}}(pd)=-0.023\times10^{-27}$ cm^2. Thus, the quark corrections to $\sigma_{\text{tot}}(pd)$ for the wave function (40)

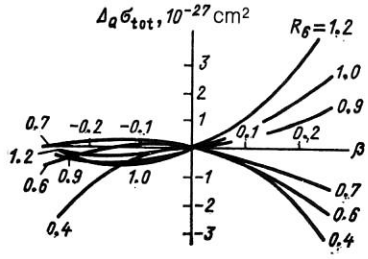

FIG. 13. Dependence of $\Delta_Q\sigma_{\text{tot}}(pd)$ on β for different values of R_6 (the numbers next to the curves).

are small and depend weakly on the form of the function $f(R)$.

The results of calculations of $\Delta\sigma_Q(pd)$ for the wave function (41) in their dependence on R_6 and β are given in Fig. 13. It can be seen that at certain values of R_6 and β the correction $\Delta_Q\sigma_{\text{tot}}(pd)$ may be very appreciable. It is interesting that $\Delta_Q\sigma_{\text{tot}}$ at $R_6=R_N$ is small and almost independent of β. Figure 14 shows the region of values of the parameters β and R_6 for which $|\Delta_Q\sigma_{\text{tot}}(pd)|<0.4\times10^{-27}$cm^2. It can be seen that at $\beta^2\gtrsim0.02$ one can obtain the estimates[48]

$$R_6\approx\begin{cases}0.7\div0.9\ \text{F}, & \beta>0;\\ 0.5\div0,95\ \text{F}, & \beta<0.\end{cases} \quad (48)$$

Note that these estimates for the radius of the S^6 state agree with the radius of the S^6 state calculated in the MIT model.[53] Indeed, it is easy to show that the mean-square radius of the S^6 state in the MIT model (for $R_{S^6}^{\text{BAG}}=1.32$ F) is equal to the rms radius of the nonrelativistic S^6 state if $R_6\sim0.87$ F.

Calculations of $T_{pd}^{2g}(q^2)$ for $q^2\neq0$ in the case of the wave function (40) with the Reid wave function $f(R)$ showed that for $q^2\lesssim0.2$ GeV^2 the difference between this amplitude and the result of the impulse approximation obtained with the same wave function $f(R)$ does not exceed 5%.

In the calculation of $T_{pd}^{2g}(q^2)$ for $q^2\neq0$ with the wave function (41) we set $R_6=0.8$ F, taking into account the estimates (48) for the radius of the S^6 state and the calculations in the MIT model. The calculations showed that the inclusion of the S^6 state can lead to an appreciable difference between $T_{pd}^{2g}(q^2)$ and the result of the impulse approximation with the same function $f(R)$. However, $F_d(q^2)$ also changes appreciably, and in the expressions of the Glauber–Sitenko approximation it is natural to use a nucleon wave function that describes the data on ed scattering. Therefore, the thing of interest is not the difference between $T_{pd}^{2g}(q^2)$ and the result of the impulse approximation obtained with the same wave function $f(R)$ but the difference between the

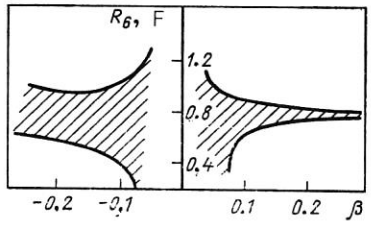

FIG. 14. Region of β and R_6 values for which $\Delta_Q\sigma_{\text{tot}}(pd)<0.4\times10^{-27}$ cm^2.

ratio $\xi = T_{pd}^{2g}(q^2)/F_d(q^2)$ and $\xi_0 = T_{pN}(q^2)/F_p(q^2)$. Clearly, $\xi = \xi_0$ if the deuteron is regarded as a pn system.

Calculations show that $|\xi - \xi_0|/\xi_0 \lesssim 0.01$ for $q^2 \lesssim 0.2$ GeV^2 and $\beta^2 \lesssim 0.1$ both, for the Reid wave function of the deuteron with a soft core and for a Gaussian wave function of the deuteron, which does not take into account the NN core at all. Thus, if we use in the expressions of the Glauber–Sitenko approximation a nucleon wave function of the deuteron that describes the data on ed scattering, this wave function must give correct results for the amplitude of hd scattering calculated in the Glauber–Sitenko approximation.

Thus, the general conclusion can be drawn that the good agreement of the Glauber–Sitenko approximation with experiment finds a natural explanation, provided that the quark wave function of the deuteron does not contain with appreciable probability a state of the type of a six-quark bag with rms radius that differs appreciably from the rms radius $R_6 \approx 0.8$ F of the S^6 state.

In this paper, we have used the wave function of the S^6 state as the wave function of the six-quark bag. There are indications[54] that states with the configuration S^4P^2 also play an important part in the interaction of nucleons at short distances. However, the situation with regard to the inclusion in the deuteron wave function of states of a six-quark bag is at present far from clear, since dynamical calculations of the deuteron wave function with allowance for S^6 and S^4P^2 states have not been made.

3.2. Double color charge exchange. Classical treatment

In the previous section we considered the effects of the color structure of the Pomeron in elastic pd scattering. The corrections were found to be small. It is clear that a contribution of the same type also exists in the diffraction dissociation $h + d \to h + X$ of the deuteron. We shall show below that the nucleon produced in this reaction can be emitted in the backward hemisphere in the laboratory system.[55] The contribution of the standard mechanisms is small in this region, and there is therefore a hope that the contribution in which we are interested is relatively enhanced.

We consider double color charge exchange of an incident hadron on the nucleons of a deuteron. If after the first color charge exchange the system of quarks of the incident hadron has gone over to a state of the color octet, then in the subsequent color charge exchange it can be made colorless with a probability of order 1/8. This corresponds to the Pomeron being attached directly to two nucleons. The deuteron, remaining colorless as a whole, goes over into a state with separated color—a color dipole. The classical trajectories of the hadron and the nucleons in such a reaction are shown in Fig. 15 in the coordinates z (longitudinal coordinate) and t (time). The decay of the color dipole here takes place by virtue of color charge exchange, in which "colored nucleons" beome white nucleons ($N_cN_c \to NN$).

The cross section for the production of a cumulative proton can be expressed in the form[55-58]

$$\frac{d^3\sigma}{dp_L\, d^2p_T} = \beta \frac{\alpha_s^2 B}{8\pi}\, e^{-Bp_T^2} (\sigma_{\text{in}}^{hN})^2\, D(L) \left(\frac{dL}{dp_L}\right) |\Psi_d(L)|^2. \tag{49}$$

Here, L is the longitudinal separation between the nucleons of the deuteron; $\Psi_d(L)$ is the deuteron wave function; p_L and p_T are the longitudinal and transverse momentum components of the cumulative proton, with L dependence of the form

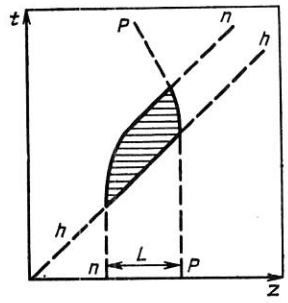

FIG. 15. Diagram describing the connection between the longitudinal coordinate z and the time t. The continuous curves show the trajectories of the colored objects, and the broken curves show those of the white objects.

$$\frac{2(E - m_N)}{2m_N - p_L - E} = \frac{\varkappa L}{m_N}, \tag{50}$$

where $E = (m_N^2 + p_L^2 + p_T^2)^{1/2}$. The parameter $\varkappa$ is the tension coefficient of the color string. For a color-triplet string, $\varkappa$ can be estimated from the meson mass spectrum[2]:

$$\varkappa = (2\pi\alpha_R')^{-1} \approx 1\,\text{GeV/F}. \tag{51}$$

The value of $\varkappa$ in the case of an octet string, in which we are interested, is unknown. For estimates in what follows, we shall use the value (51), although a larger value can be expected.[31]

The factor $D(L)$ is the probability that during the time $t = L$ the string does not "snap," i.e., there is no production of color-screening quark–antiquark pairs, no emission of gluons, etc. The function $D(L)$ has the form

$$D(L) = \exp\left[-W \int_0^t d\tau\, l(\tau)\right], \tag{52}$$

where $l(\tau)$ is the length of the string at the time τ.

The value of W can be estimated in accordance with Schwinger's formula[2] (which, strictly speaking, is not valid here), from the widths of the meson resonances,[2,3] or from the data on the multiparticle production of hadrons in e^+e^- annihilation at low energies (where, it is true, the string is not static).

The parameter W can also be estimated from the momentum spectrum of the protons in the $pp \to pX$ reaction. In the target fragmentation region, the recoil proton has a momentum equal in order of magnitude to $p \approx \varkappa\tau$, where τ is the time from the moment of color charge exchange to the first breaking of the string. The value of τ is determined by the condition $W\tau^2/2 \approx 1$ if it is assumed that the length of the color string is $l \approx \tau$ (this is true only for small values of τ; conversely, in the limit $\tau \to \infty$ we have $l \to m/\varkappa$). On the other hand, the momentum p is related to the Feynman variable x_F by $p = m_N(1 - x_F^2)/2x_F$. Since the inelasticity coefficient is $1 - \langle x_F\rangle = 0.5$, it follows that $\langle p\rangle \approx 1$ GeV. From this we find $W \approx 2/\tau^2 \approx 2\varkappa^2/p^2 \approx 2$ F^{-2}.

The quantity W determines the confinement radius—the distance to which color charges can separate. In accordance with (52), the mean length of the string is $\langle l\rangle \approx \sqrt{2/W} \approx 1$ F, i.e., of the same order as the transverse dimension.

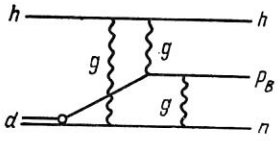

FIG. 16. Three-gluon Feynman diagram for the process $hd \to p_B hn$.

Therefore, the concept of a tube and, *a fortiori*, a string with a linear potential is very nominal.

To estimate the parameters β and B in (49), we consider the Feynman diagram in Fig. 16. This diagram does not reflect the effects of the confinement forces. However, it is natural to assume that the hadronization stage does not affect the total cross section for the reaction but merely changes the momenta of the particles in the final state. Therefore, the contribution of the diagram in Fig. 16 to the cross section for the $hd \to hpn$ reaction should be compared with the integral over p_L of the expression (49) [without the factor $D(L)$], in order to fix the parameters β and B. A calculation[55,56] yielded $\beta = 0.17$, $B = 12.8$ GeV^{-2}.

The momentum spectrum of the cumulative protons in the $pd \to p_B pn$ reaction at 180° is shown in Fig. 17. The spectrum has a maximum at $p_B \approx 0.5$ GeV.

We should add here the contributions of other mechanisms, for example, the isobaric mechanism,[60] which is important at low initial energies. At small momenta p_B, there are important contributions of spectator mechanisms, among which we may mention the model of few-nucleon correlations[61] and the part played by the large-momentum component of the nuclear structure function.[62]

Figure 17 also shows the only data that as yet exist[63] for the $pd \to p_B X$ reaction, at momentum 8.9 GeV. In order to take into account in (49) the possibility of diffraction dissociation of the incident hadron, it is necessary to introduce the factor $C_h = 1 + \sigma_{\rm DD}^{hN}/\sigma_{\rm el}^{hN}$. For protons $C_p \approx 1.4$, and for pions $C_\pi \approx 1.6$.

Comparison with the data shows that the contribution of the considered mechanism is important when $p_B \gtrsim 0.5$ GeV.

The main defect of the classical treatment is that near the kinematic boundary, $p_L \to 3m_N/4$, the internucleon separation L, which is uniquely related to p_L, increases without bound. It is clear that in a quantum-mechanical approach there is no unique connection between p_L and L. However, before we turn to the generalization of this model in quantum mechanics we study the properties of the color dipoles in the N_c–N_c system.

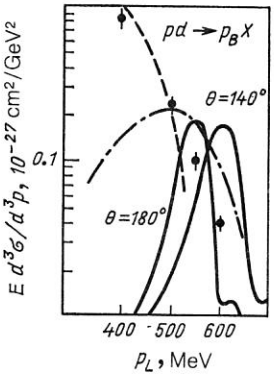

FIG. 17. Invariant cross section of the $pd \to p_B X$ reaction. The experimental points are data from Ref. 63. The continuous curves correspond to the contributions of dibaryonic resonances for scattering through angles 180 and 140°; the chain curve is the result of the classical treatment; the broken curve corresponds to the contribution of the spectator mechanism.[62]

3.3. Dibaryonic resonances with separated color. Dual properties of the scattering amplitude

We first simplify the problem and consider a system of two particles, each of which can be in two states—"white" $\binom{0}{1}$ and "colored" $\binom{1}{0}$. We write the one-dimensional Hamiltonian of such a system in the form

$$H = \frac{p_1^2}{2m} + \frac{p_2^2}{2m} + \Pi_1\Pi_2 V(x_1 - x_2) + \sigma_1\sigma_2 v(x_1 - x_2). \qquad (53)$$

Here p_1 and p_2 are the momentum operators of the particles, $\Pi_i = \binom{1\,0}{0\,0}_i$ is the projection operator onto the color state of particle i, and $V(x)$ is the confinement potential for the colored particles with relative separation x. Note that for a color string $V(x) = \varkappa|x|$. The operator $\sigma_i = \binom{0\,1}{1\,0}_i$ changes the color state of the particle. The last term in (53) corresponds to color charge exchange of the particles.

Investigating the scattering amplitude of two colorless particles NN, one can show[56,57] that the two-particle system has one bound state with negative energy (the result of the one-dimensional treatment) and a set of dibaryonic resonances in the N_cN_c system with energy $E = E_n - i\Gamma_n^{\rm el}/2$, where

$$\Gamma_n^{\rm el} = \alpha^2 |\varphi_n(0)|^2 \frac{m}{\varkappa}. \qquad (54)$$

The width $\Gamma_n^{\rm el}$ is due to the possibility of charge exchange and decay of the resonance into NN.

In the case of a linear potential $V(x) = \varkappa|x|$ the wave functions of the resonances have the form

$$\varphi_n(x) = \sqrt{\frac{\varepsilon}{2a_n'}}\,\mathrm{Ai}(\varepsilon|x| - a_n')/\mathrm{Ai}(-a_n'), \qquad (55)$$

where $\varepsilon = (2\mu\varkappa)^{1/3}$; $\mathrm{Ai}(z)$ is the Airy function; $-a_n'$ are the positions of the zeros of the derivative of the Airy function: $\mathrm{Ai}'(-a_n') = 0$.

The energy spectrum of the dibaryonic resonances has the form

$$E_n = a_n' \left(\frac{\varkappa^2}{2\mu}\right)^{1/3}. \qquad (56)$$

Snappings of the string can be taken into account by introducing an imaginary part of the potential by means of the substitution $\varkappa \to \varkappa - iW/2$, where W is the probability density for production of a $q\bar{q}$ pair, as introduced above. Making this substitution in the expression (56), we find the total width of the many particle decays:

$$\Gamma_n^{\rm in} = \frac{2W}{3\varkappa} E_n. \qquad (57)$$

With allowance for this we must make in the expression (56) the substitution $E_n \to E_n - i\Gamma_n'/2$, where $\Gamma_n' = \Gamma_n^{\rm el} + \Gamma_n^{\rm in}$ Such an approximation is valid only under the condition $\Gamma_n' \ll E_n - E_{n-1}$, and for large values of n this is not satisfied. For heavy dibaryonic resonances the lifetime becomes shorter than the time of revolution in the classical orbit, $T_{\rm cl} = 2\pi(dE_n/dn)^{-1}$, and the concept of a resonance becomes meaningless.

In the case of a linear potential it is possible to obtain an exact expression for the Green's function[56,57]

$$g_c(E;\ x,\ 0)=\frac{\mu}{\varepsilon}\,\mathrm{Ai}\left(\varepsilon\mid x\mid-\frac{\varepsilon E}{\varkappa}\right)\Big/\mathrm{Ai}'\left(-\frac{\varepsilon E}{\varkappa}\right). \qquad (58)$$

This function has the duality property. At high energies we can use the asymptotic behavior of the Airy function with complex argument, and the expression (58) takes the form of the free Green's function, this corresponding to Pomeron exchange in the scattering amplitude. At low energies, the expression (58) with $\varkappa\to\varkappa-iW/2$ has a resonance behavior. It is interesting that Pomeron–dibaryonic-resonance duality also holds on the average.[56]

We shall generalize these results to a realistic case.[56,57] The wave function of the dibaryonic resonance in the S state is modified as follows:

$$\varphi_n^{ab}(r)=\frac{\delta_{ab}}{\sqrt{8}}\,\varphi_n(r)=\frac{\delta_{ab}}{\sqrt{8}}\sqrt{\frac{\varepsilon}{4\pi}}\,\frac{\mathrm{Ai}(\varepsilon r-a_n)}{r\,\mathrm{Ai}'(-a_n)}. \qquad (59)$$

Here, allowance is made for only the possibility of nucleon charge exchange to a state of the color octet ($a, b = 1,\ldots, 8$); $a_n = 2.3,\ 4.1,\ 5.5,\ \ldots$ are the zeros of the Airy function: $\mathrm{Ai}(-a_n)=0$.

The masses of the corresponding dibaryonic resonances are

$$M_n\approx 2m+a_n\left(\frac{\varkappa^2}{2m}\right)^{1/3} \qquad (60)$$

The width of decay to the many-particle channels is given as before by the expression (57). The values of M_n and Γ_n^{in} given in Table II were calculated for the parameter values $\varkappa = 1$ GeV/F, $W = 2\ \mathrm{F}^{-2}$, and therefore they should be regarded as merely estimates. In addition, we note that a linear form of the potential $V(r)$ certainly breaks down at $r<R_0$, where R_0 is the radius of the nucleon core The modification of the potential in this region, regarded as a perturbation leads to a shift of the levels by an amount of order $\varkappa R_0$.

The expression (54) for the width of decay of the dibaryonic resonance into two nucleons is replaced by

$$\Gamma_n^{el}=\frac{mQ_n}{2\pi}\left[\int d^3\mathbf{r}\,v(\mathbf{r})\,\varphi_n(\mathbf{r})\exp(i\mathbf{Q}_n\mathbf{r})\right]^2. \qquad (61)$$

Here, $Q_n=(M_\pi^2/4-m^2)^{1/2}$ is the c.m.s. momentum of the nucleons. We estimate Γ_n^{el}. We choose the nonlocal charge-exchange potential $v(r)$ in the form

$$v(r)=v(0)\exp(-r^2/4B_{el}). \qquad (62)$$

The values of $v(0)$ and B are fixed by the NN scattering cross section: $B=B_{el}\approx 10\ \mathrm{GeV}^{-2}$, $v(0)=\sqrt{2\sigma_{in}^{NN}}/(4\pi B)\approx 0.1$ GeV.

Substituting these values of the parameters and the expression (59) in (61), we find for the first dibaryonic resonance $\Gamma_1^{el}\approx 10$ MeV. It must be emphasized that this estimate is the least reliable, since in charge exchange that takes place at low energies quark exchanges are important, and, in addition, the value of Γ_1^{el} depends exponentially on $\varkappa$, so that if $\varkappa$ is doubled Γ_1^{el} increases by almost an order of magnitude.

Note that the search for dibaryonic resonances with separated color in elastic NN scattering is hindered by the smallness of the cross section for their production. Indeed, the contribution to the dibaryonic-resonance cross section at $E_{cms}=E_n$ is $(4\pi/k^2)\Gamma_n^{el}/\Gamma_n^t$, and this is about 1% of σ_{tot}^{NN}. The process considered in the following subsection is evidently optimal for the search for dibaryonic resonances with separated color.

3.4. Cumulative process on the deuteron

We first consider the one-dimensional nonrelativistic case and generalize the Hamiltonian (53) to the case of several particles:

$$H=\sum_i\frac{p_i^2}{2m}+\sum_{i<j}\Pi_i\Pi_j V(x_i-x_j)+\sum_{i<j}\sigma_i\sigma_j v(x_i-x_j). \qquad (63)$$

We consider the scattering amplitude of three white particles: $1+2+3\to 1+2+3$. The Hamiltonian H_0, which does not contain charge exchanges, does not mix the orthogonal subspaces of states for which all particles 1, 2, 3 are white and when particle 3 is white and free while 1 and 2 are colored and interact with potential $V(x_1-x_2)$. We again regard the last term in (63) as a perturbation.

In the lowest order the three-particle scattering amplitude is shown in Fig. 18.

The amplitude for scattering of particle 1 by a "deuteron" at rest—a bound state of particles 2 and 3—has in the coordinate representation the form (in the approximation of a high energy of the incident particle 1)[56]

$$A_d=-\frac{im\alpha^3}{p_1}\int_0^\infty dx\,\Psi_d(x)\,g_c(E_{23};\ 0,\ x)\exp\left(-\frac{Wm}{8p_1}x^2\right). \qquad (64)$$

Here, E_{23} is the energy of the relative motion of particles 2 and 3. The last factor in this expression has arisen from the asymptotic behavior of the Airy function with complex argument and takes into account the prohibition on the production of $q\bar{q}$ pairs during the time of the reaction.

The physical meaning of the expression (64) is clear, namely, the potential V accelerates and brings closer together particles 2 and 3 once particle 1 has transformed them into a color dipole by two color charge exchanges. The separation between particles 2 and 3 is changed from the original x to zero, and they acquire momenta $\pm p_B$.

If the momentum p_B is sufficiently large, then in (64) we can go over to the semiclassical approximation and calcu-

TABLE II. Masses and widths of the lowest dibaryonic resonances.

n	1	2	3
M_n, GeV	2.6	3.1	3.5
Γ_n, GeV	0.2	0.35	0.5

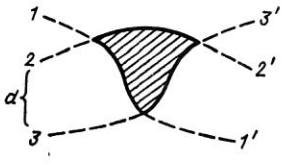

FIG. 18. Three-particle $1+2+3\to 1'+2'+3'$ scattering amplitude in the lowest order in α.

late the integral by the method of stationary phase.[56] We then obtain an expression identical to the classical expression[49] for the one-dimensional nonrelativistic problem. In this case the important longitudinal distances increase with increasing momentum, but, in contrast to the classical treatment, this growth in the expression (64) is limited by the size of the deuteron [the factor $\Psi_d(x)$] and an exponential factor. At large values of x, the stationary-phase approximation ceases to work.

With further increase of p_B the meaning of the expression (64) can be interpreted as follows. The excitation energy E'_{23} of the color dipole is made up of the work $\varkappa L$ of the color forces and the kinetic energy of the nucleons that is "prepared" in the deuteron. However, if this energy becomes too great, the two-nucleon description of the deuteron wave function becomes meaningless.

Note that in the spectator mechanism of Ref. 61 all the cumulative momentum must have been prepared in advance in the deuteron. Therefore, the region of applicability of this mechanism extends to much larger values of E'_{23} than for the spectator mechanism.

The expression (64) is modified in the realistic problem as in the previous subsection, and for the cross section of the cumulative process $hd\to p_B hn$ we obtain[56]

$$E_B\frac{d^3\sigma}{dp_B^3}=\frac{2B(\sigma_{in}^{hN})^2}{\pi Q}\left|\sum_n\frac{\sqrt{\Gamma_n^{el}}}{M-M_n+i\Gamma_n^t/2}\times\int_0^\infty dz\,\Psi_d(z)\,\varphi_n(z)\,e^{-\frac{Wz^2}{4}}\right|^2. \quad (65)$$

Here $Q=m(\alpha-1)/\sqrt{\alpha(2-\alpha)}$ is the relative momentum of the nucleons in their center-of-mass system, $M=2m/\sqrt{\alpha(2-\alpha)}$ is the effective mass of the pair, and $\alpha=(E_B+p_B^L)/m$ is a light-cone variable.

The results of calculations in accordance with (65) are shown in Fig. 17 for proton emission angles 180 and 140°. It can be seen that the curve for 180° matches well the experimental data[63] and the result of the classical approach.[55] It can also be seen that the angular dependence varies strongly with increasing p_B. Generally speaking, we have the following scaling: For a fixed value of α the cross section does not depend on the angle.

Observation of dibaryonic resonances in a cumulative process at large values of p_B appears to be optimal from the point of view of the possible physical background, since it is difficult to find a mechanism that makes an appreciable contribution in this region of cumulative momenta. The contribution of a spectator mechanism, if there is one, can be suppressed by separating the diffraction process or by simply studying the reaction $hd\to p_B hn$.

Although the contribution of the present mechanism does depend on the energy at higher energies, there is a specific dependence at intermediate energies. The Green's function of the system consisting of the incident proton and a target nucleus has a resonance dependence on $E_{12}=(2mT_{kin}+4m^2)^{1/2}-2m$, where T_{kin} is the kinetic energy of the incident proton. If it is assumed that the mass of the first dibaryonic resonance is 3 GeV, then the first maximum in the energy dependence must occur at $T_{kin}\approx 2.6$ GeV. Actually, the mechanism, which only begins at this energy, makes an appreciable contribution to the cross section of the cumulative process.

We note also that if the incidemt particle is a pion, then the resonances in the function $g_c(E_{12})$ are pion–nucleon five-quark resonances with separeted color. The excitation spectrum of these resonances is close to a dibaryonic spectrum.

3.5. Backward elastic *pd* scattering

At intermediate energies in the $pd\to p_B pn$ reaction, the proton and neutron, emitted forward, can have momenta that are comparable in magnitude and form a bound state—the deuteron. The corresponding graph is shown in Fig. 19. If the Green's function is represented as a sum over resonances, and the momentum distribution of the nucleons in the deuteron is ignored, the following expression can be obtained for the cross section[56,57]

$$\frac{d\sigma}{d\Omega}=\frac{25}{18}\frac{|\Psi_d(0)|^2}{Q^2}\times\left|\sum_{n,n'}\frac{\sqrt{\Gamma_n^{el}\Gamma_{n'}^{el}}F_{nn'}(\mathbf{p},\mathbf{p}')}{(M-M_n+i\Gamma_n^t/2)(M-M_{n'}+i\Gamma_{n'}^t/2)}\right|^2, \quad (66)$$

where $F_{mm'}(\mathbf{p},\mathbf{p}')$ is the amplitude for backward scattering of a dibaryonic resonance, $n\to n'$, by a nucleon,

$$F_{nn'}(\mathbf{p},\mathbf{p}')=\int d^3\mathbf{r}\,d^3\mathbf{r}'\,\varphi_n(\mathbf{r})\,V(\mathbf{r}-\mathbf{r}')\,\varphi_{n'}(\mathbf{r}')\times\exp\left[i\frac{\mathbf{r}}{2}\left(\mathbf{p}'+\frac{\mathbf{p}}{2}\right)-i\frac{\mathbf{r}'}{2}\left(\mathbf{p}+\frac{\mathbf{p}'}{2}\right)\right].$$

The result (66) has a transparent interpretation (Fig. 19). When the incident proton collides with a target nucleon, a dibaryonic resonance is formed with probability proportional to Γ_n^{el}. It is then scattered through 180° by the second nucleon of the deuteron by stripping of the colored nucleon. It is interesting that this process takes place at a smaller c.m.s. momentum, equal to $\sim p/2$.

To estimate the cross section, we ignore in (66) the terms with $n\neq n'$ and the dependence of F_{nn} on n, calculating only F_{11}. The result of the calculation is shown in Fig. 20. The overall normalization of the cross section depends quadratically on Γ_n^{el} and is chosen, to within the uncertainty noted above in the value of Γ_n^{el}, in accordance with the experimental data.[64] As can be seen in Fig. 20, the experimen-

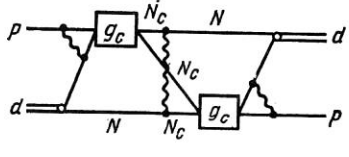

FIG. 19. Feynman diagram for backward elastic *pd* scattering.

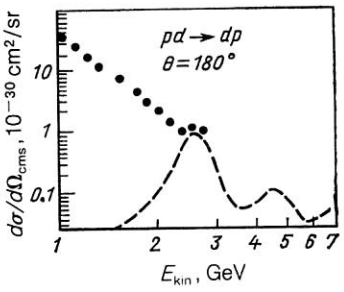

FIG. 20. Differential cross section for backward elastic *pd* scattering as a function of the kinetic energy of the protons in the center-of-mass system. The experimental data are from Ref. 64, and the broken curve demonstrates the calculation in accordance with the expression (66) (see the text).

tally observed change in the energy dependence of the curve at $T_{\text{kin}} \approx 2.5$ GeV can be attributed to the contribution of a dibaryonic resonance with a mass around 3 GeV. It can be seen from the figure that the contribution of this mechanism at lower energies is negligibly small.

We emphasize once more that the masses of the dibaryonic resonances given in Table II are estimates. They depend strongly on the value of $\varkappa_8$ for the octet string and have been obtained for the case $\varkappa_8 = \varkappa_3 = 1$ GeV/F. In the MIT model,[65] for example,

$$\varkappa_8 = (3/2)\,\varkappa_3,$$

and for the lowest dibaryonic resonance we obtain $M_1 = 2.8$ GeV.

Here, however, we have assumed universality of the parameter B, the jump in the vacuum energy density across the bag surface; for octet strings (elongated bags) this is apparently incorrect.[66] The value of $\varkappa_8$ can be estimated[31] from the relation (51) by replacing in it $\alpha'_R \approx 0.9$ GeV^{-2} by $\alpha'_P \approx 0.15$–0.25 GeV^{-2}, this giving $\varkappa_8 \approx (4-6)\varkappa_3$ and, accordingly, $M_1 \approx 3.5$–4 GeV.

Another source of uncertainty in the masses of the dibaryonic resonances is the fact that the three-quark cluster is a color octet formed from a nucleon by single-gluon exchange, and it cannot be in the S state. Therefore, its mass m in the expression (60) may be greater than the nucleon mass.

It should also be noted that the dibaryonic resonance has a further decay channel that we have not considered above. The octet tube may divide not only "transversely" but also "longitudinally," decaying into three triplet tubes. This decay channel increases Γ^t_n, but it is not possible to estimate its contribution. In models of dual topological unitarization it is assumed for simplicity that in place of an octet string two triplet strings are always formed, this corresponding to $\Gamma^t_n/\Delta E_n \gg 1$, i.e., in such models dibaryonic resonances do not occur. The integrated contribution to the cross section of the cumulative process is unchanged. Only the shape of the momentum spectrum in Fig. 17 is changed, being in this limit close to the result of the classical treatment.

4. CONSEQUENCES OF THE SPACE-TIME STRUCTURE OF HADRON PRODUCTION PROCESSES

4.1. Production of J/Ψ mesons and lepton pairs on nuclei

It is usually assumed that hard processes in hadron–nucleus collisions are not screened, since their cross section is small, while the soft inelastic collisions in the nucleus do not influence the hard parton component of the incident hadron. However, this is valid only far from the kinematic limit. For the mean momentum of the leading hadron in a soft inelastic collision is about half the initial momentum, and such a hadron could not in a secondary "hard" collision produce a particle near the kinematic limit. Therefore, the hard process is screened by the soft process.[67] However, this conclusion applies to macroscopically large distances between the two targets. At distances of a few fermis after the inelastic interaction the spectrum of the leading hadrons can be calculated only in a definite model.

Let $\varkappa_{\text{eff}}$ be a parameter that characterizes the fragmentation "rate": Over the interval Δz from the point of the color charge exchange, hadrons with momenta $p \lesssim \varkappa_{\text{eff}} \Delta z$ are produced. The harder part of the hadron wave function of the incident hadron, preserving its coherence; has momentum $\varkappa_{\text{eff}} \Delta z$ less than the momentum p_0 of the incident hadron, i.e., it can subsequently fragment only into hadrons with momenta $p < p_0 - \varkappa_{\text{eff}} \Delta z$. Bearing this in mind, we can readily calculate the degree of screening of the deep nucleons of a nucleus.

Let us consider J/Ψ production in hA interaction.[68] We denote by E the energy of the hadron h, and by $x_F = 2p_L^{\Psi}/\sqrt{s}$ the Feynman variable of the J/Ψ meson for the hN collision. We represent the cross section σ_{Ψ}^{hA} as the sum $\sigma_{\Psi}^{hA} = \sigma_1^{hA}(E, x_F) + \sigma_2^{hA}(E, x_F)$. The first term corresponds to the incident hadron forming a J/Ψ on one of the nucleons of the nucleus without having undergone a single inelastic interaction before this happens. Such events occur on the surface of the nucleus, and their contribution is

$$\sigma_1^{hA}(E,\ x_F) = \int \mathrm{d}^2\mathbf{b} \int_{-\infty}^{\infty} dz\, \rho(\mathbf{b}, z)\, \mathrm{e}^{-\sigma_{\text{in}}^{hN} T(\mathbf{b},\, -\infty,\, z)} \times \frac{1}{2}\{\sigma_{\Psi}^{hp}(E,\ x_F)[1-\delta(\mathbf{b}, z)] + \sigma_{\Psi}^{hn}(E,\ x_F)[1+\delta(\mathbf{b}, z)]\} \times \mathrm{e}^{-\sigma_{\text{in}}^{\Psi N} T(\mathbf{b},\, z,\, \infty)}. \quad (67)$$

Here $\delta(\mathbf{b}, z) = (\rho_n - \rho_p)/2\rho$ is the relative difference between the densities of the neutrons and protons; σ_{in}^{hN} is the inelastic cross section of the hN interaction; $\sigma_{\text{in}}^{\Psi N} \approx 2.2 \times 10^{-27}$ cm^2 is associated mainly with the channel $\Psi N \to D\bar{D}X$. The contribution of the $\Psi N \to \Psi X$ process is small, about 0.08×10^{-27} cm^2.

The second term $\sigma_2^{hA}(E, x_F)$ corresponds to the fact that the incident hadron has undergone one or more color charge exchanges and has reduced its energy to $\tilde{E}$:

$$\sigma_2^{hA}(E,\ x_F) = \int d^2\mathbf{b} \int_{-\infty}^{\infty} dz_1\, \rho(\mathbf{b}, z_1)\, \mathrm{e}^{-\sigma_{\text{in}}^{hN} T(\mathbf{b},\, -\infty,\, z_1)} \int_{z_1}^{z_1 + \frac{E'}{\varkappa}(1-x_F)} dz_2 \times \rho(\mathbf{b}, z_2)\, \frac{1}{2}\{\sigma_{\Psi}^{hp}(\tilde{E},\ \tilde{x}_F)[1-\delta(\mathbf{b}, z_2)] + \sigma_{\Psi}^{hn}(\tilde{E},\ \tilde{x}_F)[1+\delta(\mathbf{b}, z_2)]\}\, \mathrm{e}^{-\sigma_{\text{in}}^{\Psi N} T(\mathbf{b},\, z_2,\, \infty)}. \quad (68)$$

Here, we have taken into account the energy shift $\tilde{E} = E - \varkappa \Delta z$ with respect to the Feynman variable $\tilde{x}_F = x_F(1 - \varkappa \Delta z/E)^{-1}$, $\Delta z = z_2 - z_1$ as well.

Since the dependence of σ_{Ψ}^{hN} on the transverse dimension of the hadron is unknown, we estimated the cross sec-

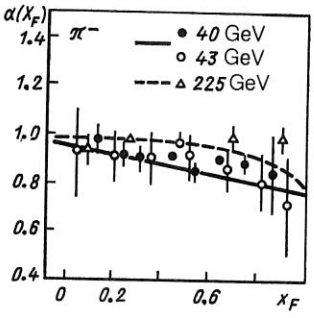

FIG. 21. Exponent α that characterizes the A dependence of the cross section (A^{α}) for J/Ψ production on nuclei as a function of the Feynman variable x_F.

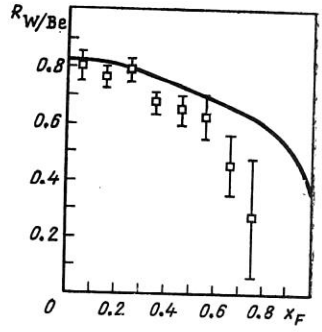

FIG. 23. Ratio $R = (d\sigma_W/dx_F)/(d\sigma_{Be}/dx_F)$ of the cross sections for J/Ψ production on the W and Be nuclei in a π^- beam with energy 125 GeV. The data are from Ref. 73.

tion in the Glauber–Sitenko approximation, ignoring the inelastic corrections.

The contributions $\sigma_2^{hA}(E, x_F)$ increases almost as A at small x_F and a $A^{2/3}$ in the limit $x_F \to 1$. This is confirmed by the experimental data[69–71] for the exponent $\alpha(x_F)$ given in Fig. 21, and also by data[71,72] for the x_F dependence of the ratio $\sigma_\Psi^{hp}(E, x_F)/\sigma_\Psi^{hA}(E, x_F)$, which are given in Fig. 22. Also shown there are the results of calculations in accordance with the expressions (67) and (68). The difference between the cross sections $\sigma_\Psi^{\pi^\pm p}$, which amounts to a few percent,[72] was ignored. The energy dependence $\sigma_\Psi^{hN}(E)$ was represented in the form (Ref. 71) $\sigma_\Psi^{hN}(E) \propto \exp(-\beta\sqrt{E})$, where $\beta \approx 2$ GeV. The dependence of σ_Ψ^{hp} on x_F was represented in the form $\sigma_\Psi^{hp}(x_F) \propto (1-x_F)^2$, $\sigma_\Psi^{pp}(x_F) \propto (1-x_F)^5$. The value of $\varkappa \equiv \varkappa_{\text{eff}}$ was varied, and the best agreement was achieved for $\varkappa \approx 3$ GeV/F.

Allowance for the Fermi motion in the nucleus partly compensates the influence of deceleration. Estimates made at 40 GeV showed that the corrections are small[71] and decrease rapidly with increasing energy.

Note that the difference between the x_F dependences of the data in Fig. 22b for proton and pion beams confirms that the effect is associated with the deceleration of the hadron in the nucleus, since the x_F dependence of σ_Ψ^{pp} is steeper than that of $\sigma_\Psi^{\pi p}$. This is also confirmed by comparison of the data in Figs. 22a and 22b, from which it can be seen that with increasing energy the nuclear screening occurs at larger values of x_F.

The effect of nuclear screening in the production of J/Ψ in a $\hat{p}$ beam with energy 125 GeV has also been observed.[73] The authors, having considered various possible explanations of the effect, concluded that only a calculation made in the present approach agrees with the data. The corresponding comparison is made in Fig. 23.

To conclude this subsection we note that the graph corresponding to the considered mechanism is a planar three-Reggeon graph.[74] It must be distinguished from nonplanar Mandelstam graphs containing a three-Pomeron vertex. These graphs correspond to an additional screening that has the same nature as the inelastic screening of the total hadron–nucleus cross sections. In a frame of reference in which the nucleus is fast there is longitudinal overlapping and fusion of the parton clouds[11] of different nucleons, and this reduces the number of slow partons, i.e., it leads to screening.

The contribution of the planar three-Reggeon graphs at a given value of x_F is large only in the restricted range of energies $E \leqslant n x_F (1-x_F)^{-1} \varkappa R_A$, where $n \approx 2$ for incident pions and $n \sim 5$ for nucleons. As the energy is increased, this correction is shifted to the region of larger x_F, $x_F \to 1$, and disappears.

In contrast, the screening due to the nonplanar graphs appears only at sufficiently high energies $E \gg M_\Psi^2/mx_F$. With increasing energy the region of x_F values in which this correction is important extends to smaller x_F, and in asymptotia the cross section is $\sigma_\Psi^{hA}(E \to \infty) \propto A^{2/3}$ for all values of x_F.

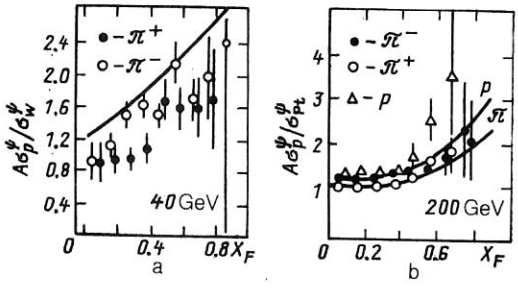

FIG. 22. Normalized ratio of cross sections of J/Ψ production on hydrogen and tungsten in π^+ and π^- beams at 40 GeV (a) and for the platinum nucleus at 200 GeV in π^+, π^-, and p beams (b).

4.2. Fragmentation time at the boundary of the kinematic region

In the old parton model[74] (constructed in the spirit of $\lambda\varphi^3$ field theory) it is assumed that the produced hadrons are incapable of interacting until they have formed a parton cloud containing slow partons. This requires a time

$$l_f \approx p/\mu^2, \tag{69}$$

where p is the hadron momentum, and μ is a mass parameter of order m_ρ. Allowance for the formation time of the wave function of the hadron, during which it is passive, has a strong effect on the generation of hadrons on nuclear targets.[74]

In QCD any produced objects can immediately interact by exchanging a Coulomb gluon. However, when a color charge fragments, a hadron with momentum p is not produced immediately but only at distance $l_f \approx p/\varkappa$, and this corresponds to the result (69) of the parton model, since, as was shown in the previous section, $\varkappa_{\text{eff}} \approx m_\rho^2$. At the same time, it is important that although the color charge is capable

of interacting over the interval l_f, this has little influence on the spectrum of the leading hadrons.[75]

A difference from the dependence (69) arises for the leading hadrons when $\beta > \bar{\beta}$, where β is the fraction of the initial momentum of the color charge carried away by the hadron. A hadron with $\beta > \bar{\beta}$ must be produced at distance[75,36]

$$l_f \approx \frac{p_0}{\varkappa_{\text{eff}}}(1-\beta). \tag{70}$$

Indeed, at greater distances $\Delta z > l_f$ the color charge, having lost momentum $\Delta p = \varkappa_{\text{eff}} \Delta z$ on the production of hadrons, is incapable of fragmenting into a hadron with momentum βp_0.

Thus, near the kinematic limit as $\beta \to 1$ the fragmentation length of the leading hadron does not increase but decreases with increasing momentum in accordance with (70). It should be emphasized that this is not the time of formation of the hadron wave function, which, of course, increases in accordance with (69). The fragmentation time (70) is the time during which the screening of the color charge takes place. The produced colorless cluster ($q\bar{q}$, for example) is not yet a hadron, but this cluster can interact inelastically with a cross section of the order of the hadron cross section.

4.3. Production of symmetric pairs of hadrons with large p_T on nuclei

When there is inclusive production of hadrons with large p_T on nuclei, appreciable antiscreening, which has become known as the Cronin effect,[76] is observed. The main reason for this is evidently multiple scattering of hard partons in the nucleus. This can be verified by separating the single hard process by detecting a symmetric pair of hadrons with large p_T.[77] A linear A dependence was indeed observed[78] with such an arrangement. However, in the experiment of Ref. 79 at 70 GeV it was found that with increasing p_T of the symmetric meson pairs the exponent $\alpha(p_T)$ that describes the A dependence $A^{\alpha}(p_T)$ fell sharply. This can be seen in Fig. 24.

The strong screening appears in the single process at large p_T for a reason similar to that considered in the previous subsection, except that, in contrast to J/Ψ production, in the present case an important contribution is made by the possibility of absorption of the produced hadrons in the nucleus. By absorption we mean an inelastic interaction, i.e., color charge exchange of the produced colorless hadron state, as a result of which hadronization recommences and the hadron loses an appreciable fraction of the momentum. The hadron with large p_T is produced as a result of hadronization of a quark scattered with large transverse momentum transfer. The quark–hadron fragmentation length l_f is given by the expression (70). We ignore the possible dependence of $\varkappa_{\text{eff}}$ on p_T.

In the limit $x_T \to 1$ ($x_T \approx 2p_T/\sqrt{s}$) we also have $\beta \to 1$, i.e. $l_f \to 0$. Therefore, the hadron is produced immediately after the hard scattering of the quark and can be absorbed by the nucleus. It follows from this and from the previous subsection that the cross section for the production of a hadron with large p_T on a nucleus (in the case of a single hard scattering) depends on A as $A^{1/3}$ in the limit $x_T \to 1$.

We shall write an expression for the cross section $\sigma_{\text{inv}}(x_T) \equiv E_1 E_2 d\sigma/d^3p_1 d^3p_2$ for the production of a symmetric pair of hadrons produced at angle 90° in the center-of-mass system of the nucleon–nucleon collision. We denote by α_1 and α_2 the fractions of the momenta of the initial nucleons associated with the scattered quarks, and by β_1 and β_2 the fractions of the momenta of these quarks carried away after their fragmentation by the leading hadrons. Then in the NN collision

$$\sigma_{\text{inv}}(x_T) = C \int d\alpha_1\, d\alpha_2\, d\beta_1\, d\beta_2 F(\alpha_1) F(\alpha_2) \times D(\beta_1) D(\beta_2)\, \sigma_{qq}(\alpha_1\alpha_2 s)\, \delta(x_T - \alpha_1\beta_1)\, \delta(x_T - \alpha_2\beta_2).$$

Here, $F(\alpha)$ is the momentum distribution function of the quarks in the nucleon, which we take in the form $F(\alpha) \propto (1-\alpha)^3/\sqrt{\alpha}$. We use the quark fragmentation function in the form $D(\beta) \propto (1-\beta)^2/\beta$. We write the cross section for elastic scattering of the quarks in the form corresponding to single-gluon exchange, $\sigma_{qq}(Q) \propto 1/Q^4$; C is a constant that is of no importance in what follows. If we ignore the transverse momenta of the quarks in the initial nucleons and hadrons in the final jets, then $\alpha_1 \approx \alpha_2 \equiv \alpha$, $\beta_1 \approx \beta_2 \equiv \beta$, $x_T \approx \alpha\beta$.

In the case of a nuclear target, we separate, as in the case of J/Ψ two contributions to the cross section for the production of a symmetric pair of hadrons: $\sigma_1^{\text{inv}}(x_T)$ corresponds to the incident hadron not undergoing any inelastic collision before the hard scattering; $\sigma_2^{\text{inv}}(x_T)$ includes one or more soft color charge exchanges of the initial hadron:.

$$\sigma_1^{\text{inv}}(x_T) = C \int d^2\mathbf{b} \int_{\infty}^{\infty} dz\, \rho(\mathbf{b}, z)\, e^{-\sigma_{\text{in}}^{NN} T(\mathbf{b}, -\infty, z)} \times \int_{x_T}^{1} d\alpha F^2(\alpha)\, D^2\left(\frac{x_T}{\alpha}\right) \alpha^{-2} \sigma_{qq}(\alpha^2 s)\, e^{-(\sigma_{\text{in}}^{h_1 N} + \sigma_{\text{in}}^{h_2 N}) T(\mathbf{b}, z+l_f, \infty)}; \tag{71}$$

$$\sigma_2^{\text{inv}}(x_T) = C \int d^2\mathbf{b} \times \int_{-\infty}^{\infty} dz_1\, \sigma_{\text{in}}^{NN} \rho(\mathbf{b}, z_1)\, e^{-\sigma_{\text{in}}^{NN} T(\mathbf{b}, -\infty, z_1)} \int_{z_1}^{\infty} dz_2 \rho(\mathbf{b}, z_2) \times \int_{\tilde{x}_T}^{1} d\alpha F^2(\alpha)\, D^2\left(\frac{\tilde{x}_T}{\alpha}\right) \alpha^{-2} \sigma_{qq}(\alpha^2 \tilde{s}) e^{-(\sigma_{\text{in}}^{h_1 N} + \sigma_{\text{in}}^{h_2 N}) T(\mathbf{b}, z+\tilde{l}_f, \infty)} \tag{72}$$

We have here introduced the notation $s = 2m_N^2 + 2m_N \tilde{E}$, $\tilde{E} = E - \varkappa(z_2 - z_1)$, $\tilde{x}_T = 2p_T/\sqrt{\tilde{s}}$, $l_f = E(\alpha - x_T)/2\varkappa$, $\tilde{l}_f = \tilde{E}(\alpha - \tilde{x}_T)/2\varkappa$.

The calculation in accordance with the expressions (71) and (72) of the exponent $\alpha_{12}(x_T) = d\ln[\sigma_1^{\text{inv}}(x_T) + \sigma_2^{\text{inv}}(x_T)]/d\ln A$ for $A = 100$, $E = 70$ GeV, $\varkappa = 3$ GeV/F is shown in Fig. 24 by the broken curve. It can be seen that with increasing p_T the exponent $\alpha_{12}(x_T)$ falls to $\frac{1}{2}$.

A hadron pair can also be produced by a different mechanism—the statistical mechanism, in which the hadrons are produced independently and randomly appear in corresponding regions of the phase space. The contribution to the cross section of this mechanism is

$$\sigma_3^{\text{inv}}(x_T) = E_1 \frac{d^3\sigma}{d^3p_1} E_2 \frac{d^3\sigma}{d^3p_2} \Big/ \sigma_{\text{in}}^{NA}. \tag{73}$$

The A dependence of $\sigma_3^{\text{inv}}(x_T)$ is characterized by an exponent $\alpha_3(x_T) = d\ln[\sigma_3^{\text{inv}}(x_T)]/d\ln A \approx \alpha_{h1}(x_T)$

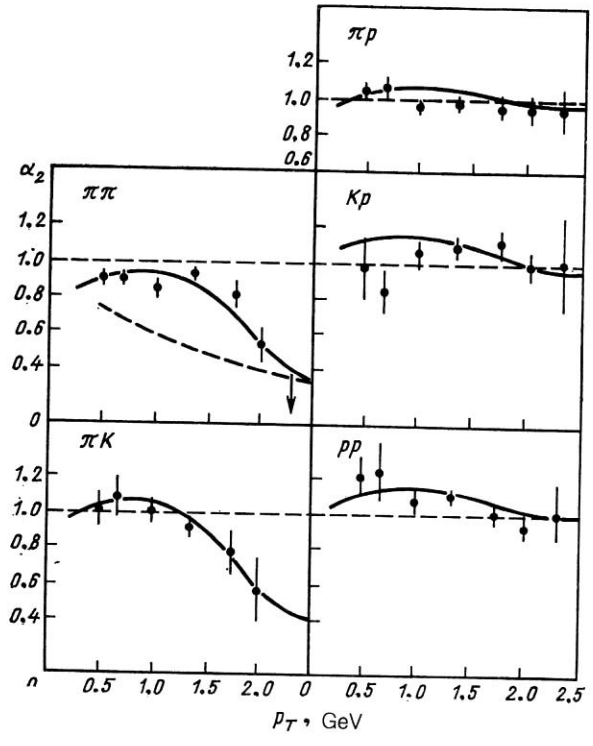

FIG. 24. Dependence of the exponent α on p_T in processes with production of symmetric hadron pairs on nuclei at 70 GeV.

$+\alpha_{h2}(x_T) - 2/3$. Here, $\alpha_h(x_T)$ is the exponent in the A dependence for the inclusive production of hadron h on the nucleus. The values of $\alpha_h(x_T)$ for different hadrons were measured in the special experiment of Ref. 80.

It is clear that the statistical mechanism makes a significant contribution at values of p_T that are not very large. This is confirmed by the results of measurement[81] of the correlation function, which is constant and of order unity for $p_T \lesssim 0.7$ GeV/c and increases sharply at large p_T. The contribution of the statistical mechanism is also manifested in the p_T dependence of the pair production cross section, which can be approximated by two exponentials[81]:

$$\sigma_{NN}^{\text{inv}}(x_T) = he^{-Hp_T} + re^{-Rp_T}. \qquad (74)$$

The values of the parameters h, H, r, R used later in the calculations are assumed to be independent of the species of the produced hadrons and are fixed in accordance with the data of Ref. 81 by the values $r/h = 0.006$ and $R - H = 6$ $(\text{GeV}/c)^{-1}$.

The first term in (74) corresponds to the hard pair-production mechanism, and the second to the statistical mechanism. Accordingly,

$$\alpha_{\text{eff}}(x)_T = \frac{\alpha_{12}A^{\alpha_{12}} + (r/h)\,\alpha_3 A^{\alpha_3} e^{(H-R)p_T}}{A^{\alpha_{12}} + (r/h)\,A^{\alpha_3} e^{(H-R)p_T}}.$$

Results of the calculation of $\alpha_{\text{eff}}(x_F)$ for $\pi^+\pi^+$ and π^+K^+ pairs are shown in Fig. 24 by the continuous curves. It can be seen that the sharp decrease in $\alpha_{\text{eff}}(x_T)$ at $p_T \gtrsim 1$ GeV is due to the transition from the statistical to the hard hadron-production mechanism.

It is important that the experimental data agree well with $\varkappa_{\text{eff}} = 3$ GeV/F. Note that the Fermi motion and the collective interaction mechanisms, which in the inclusive arrangement can strongly increase $\alpha(x_T)$ as $x_T \to 1$, are strongly suppressed in the case of the production of symmetric pairs by the kinematics of such events.

With increasing energy the region of the nuclear screening is shifted to larger values of p_T. Figure 25 shows the results of measurements[82] at energies 400 and 800 GeV and calculations made in Ref. 85 in the present approach. The agreement is good.

Events with the production of nucleon or meson–nucleon pairs warrant special discussion. It can be seen from the data of Ref. 79, shown in Fig. 24, that in these events $\alpha_{\text{eff}}(x_T)$ does not deviate from unity to within the errors.

To understand the reason for this, we recall that at energy 70 GeV protons with large p_T are produced in the inclusive arrangement with a cross section significantly larger than for pions.[80,81]

This fact can be interpreted by saying that the protons are produced, not as pions as a result of fragmentation, but by scattering of the system of three valence quarks of the initial nucleons (of the beam or the nucleus).

The absence of nuclear screening in the production of pp pairs can be understood in this case. The single-gluon exchange in the scattering of the $3q$ system selects small dimensions $\tau \approx 1/q$, and such configurations are weakly absorbed in the nucleus. As a result, we must substitute $\alpha_{12} = 1$ in the expression (75). The result of the calculation for a pp pair is shown in Fig. 24.

Nevertheless, the existing data do not yet permit us to conclude that this mechanism of production of proton pairs

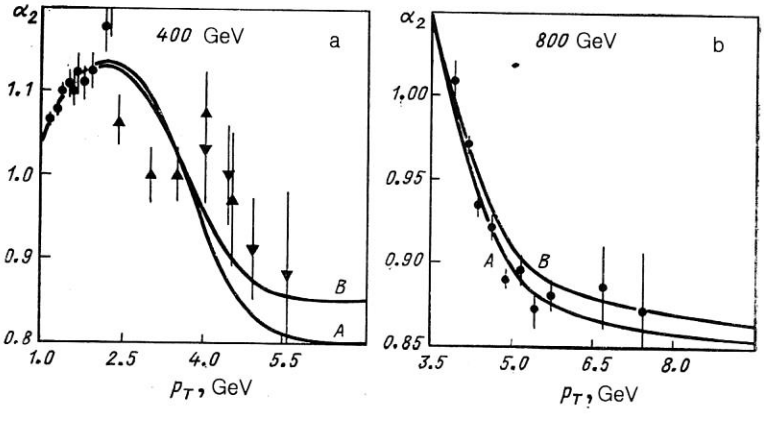

FIG. 25. The same as in Fig. 24 at the energies 400 GeV (a) and 800 GeV (b): curve A is for $\varkappa = 3$ GeV/F, and curve B for $\varkappa = 2$ GeV/F.

is the dominant one. The contribution from the scattering of small, $r_D \sim 0.3$ F, diquarks, considered in Ref. 85, can also explain the data.[79]

In conclusion, we note that for $x_T \ll m_\pi/m_N$ there is an additional inelastic screening in the structure function of the nucleus considered in the previous subsection. It leads to a decrease of α_{eff} to 2/3 at small x_T. Because of the contribution of the statistical mechanism, this effect can be manifested only at very high energies.

4.4. Fragmentation time and nuclear screening of inclusive reactions in the three-Reggeon region

At high energies we restrict ourselves to the contribution to the inclusive reaction cross section of the scaling three-Reggeon *RRP* and *PPP* graphs. The first of them has already been discussed in Sec. 2.6 and is shown in Fig. 11. The nuclear screening of the contribution of this graph was calculated in accordance with the expression (38), in which the effects of the fragmentation time were ignored. This was justified by the smallness of the energy (10 GeV), corresponding in the three-Reggeon region to fragmentation times less than 1 F. At high energies l_f increases and must be taken into account in the calculation of A_{eff}:

$$A_{\text{eff}}(x_F) = \int d^2\mathbf{b} \int_{-\infty}^{\infty} dz\, \rho(\mathbf{b}, z) \left| \left\langle \frac{|f(q, \tau)}{\langle f(q, \tau)\rangle} \right. \right.$$
$$\times \exp\left\{ -\frac{1}{2}\sigma(\tau)\left[T(\mathbf{b}) - \int_z^{z+l_f} dz'\, \rho(\mathbf{b}, z') \right] \right\} \Big\rangle \Big|^2. \quad (75)$$

As in (38), we take $f(\tau) \propto \tau^2$, $\sigma(\tau) \propto \tau^2$, and the hadron wave function in the Gaussian form; we obtain

$$A_{\text{eff}}(x_F) = \int d^2\mathbf{b} \int_{-\infty}^{\infty} dz\, \rho(\mathbf{b}, z) \left[1 + \frac{1}{2}\sigma_{\text{tot}}^{hN} T(\mathbf{b}) \right.$$
$$\left. - \frac{1}{2}\sigma_{\text{tot}}^{hN} \int_z^{z+l_f} dz'\, \rho(\mathbf{b}, z') \right]^{-4}. \quad (76)$$

The expression (37) is modified similarly. Figure 12 shows the predictions for the ratio $R_{\text{Cu}/d}(x_F)$ at energy 40 GeV. It can be seen that the decrease in the contribution of the RRR graph and the influence of the hadronization time have appreciably changed the dependence $R_{\text{Cu}/d}(x_F)$.

We now consider the three-Pomeron graph. Its space–time structure is shown schematically in Fig. 26. The hadron fluctuation incident on the target is a coherent system of quarks and gluons ordered in rapidity. As a result of color exchange with the target, the fast part of the quarks and gluons, carrying momentum fraction x_T of the incident hadron, is made colorless and forms into a hadron. The remaining gluons in the soft part of the spectrum fragment into hadrons.[86]

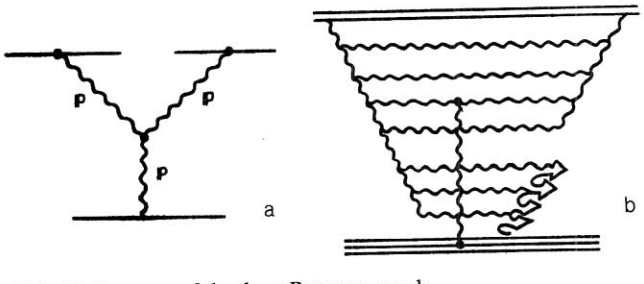

FIG. 26. Structure of the three-Pomeron graph.

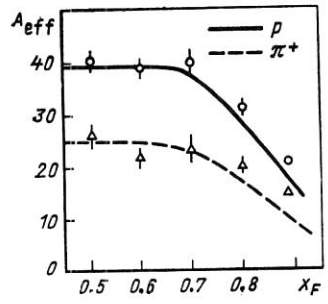

FIG. 27. $A_{\text{eff}}(x_F)$ for the cross sections of the reactions $pA \to pX$ and $\pi A \to \pi X$, integrated over p_T, at energy 100 GeV.

If this process takes place on a nucleon in the nucleus at the point with longitudinal coordinate z_1, then the inelastic interactions of the incident hadron with nucleons at $z < z_1$ do not necessarily screen it. Indeed, if $\Delta z < (1 - x_F)p_0/\varkappa$, then on this interval the coherence of the gluons in the soft part of the spectrum is lost, while the system of quarks and gluons with momenta $p > p_0(1 - x_F)$ remains coherent and, becoming colorless, can become a hadron.

With allowance for the absence of screening before interaction on an interval Δz identical to (70), it is necessary to calculate A_{eff} for the three-Pomeron graph using the same expressions (75) and (76) as for the *RRP* graph.

Thus, in the diffraction process $hA \to hK$ in which the hadron composition is not changed, the screening in the nucleus is weakened to the same extent as in the process with charge exchange, although the reasons for this are different. At the same time, of course, there is no weakening of the nuclear interaction (apart from the inelastic corrections) in the process of the diffraction dissociation of the incident hadron.

The strong dependence of l_f on x_F in Eqs. (75) and (76) must lead to a decrease of $A_{\text{eff}}(x_F)$ with increasing x_F in the three-Reggeon region.[36,75] This effect has indeed been observed[87] in reactions of the type $\pi^+ A \to \pi^+ X$ and $pA \to pX$ at 100 GeV. In Fig. 27 the results of a calculation of A_{eff} in accordance with (76) with $\varkappa_{\text{eff}} = 3$ GeV/F are compared with the data of Ref. 87.

4.5. Absorption of hadrons by the nuclear medium in tunneling from the vacuum

It is assumed[2,3] that in soft processes particles are produced from the vacuum by virtue of the work of the forces of the external field. The greater the mass of the produced particles, the longer the below-barrier transition that they must make. A particle–antiparticle pair produced in an external field from the vacuum goes onto the mass shell at relative distance $\Delta z = 2m/\varkappa$, where m is the mass of the particle, and $\varkappa$ is the work done by the external field over unit length. In the case of a string, $\varkappa$ is the tension coefficient. For subsequent estimates we take $\varkappa = 1$ GeV/F, since this case is close to the stationary problem. In this case the $N\bar{N}$ pair produced from the vacuum appears at a relative distance $\Delta z \sim 2$ F in the center-of-mass system. If we go over to the laboratory system, then the p and the $\bar{p}$ appear at different times and at different distances from the target.[88] The particle that is first in time appears at distance ~ 1 F, and the second at distance

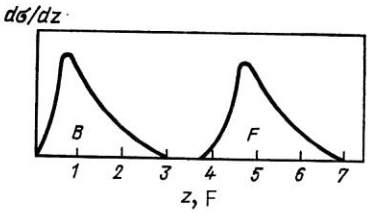

FIG. 28. Distribution with respect to the longitudinal coordinate in the laboratory system of the produced $\bar{p}$ at initial momentum 10 GeV.

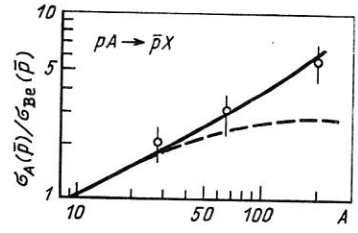

FIG. 29. Cross section for production of $\bar{p}$ on nuclei, normalized to ^{9}Be. The continuous curve is the calculation in accordance with (78), and the broken curve corresponds to the calculation of Ref. 90 with $l_f = 0$. The data are from Ref. 90.

~5 F. If the energy of the incident nucleon is above the threshold value, then there is a distribution over the distances at which the p and $\bar{p}$ appear. An example of such a distribution for initial momentum 10 GeV is shown in Fig. 28, where F and B represent the particles (it is immaterial whether p or $\bar{p}$) produced in the center-of-mass system forward or backward with respect to the beam direction.

This conclusion can be verified in an experiment by means of the interference method.[89] Since the p and $\bar{p}$ momenta are nearly equal in value, the longitudinal separation between the production points can be measured. If the tunneling occurs in an absorbing medium (a nucleus), we can ask how the absorption affects the tunneling probability The answer is, very weakly.

We consider tunneling in the one-dimensional nonrelativistic case in the semiclassical approximation. The semiclassical exponential $\exp[i/h \int^z dz' p(z')]$, where $p^2(z) = 2m[E - v(z)]$, decreases with increasing z in the below-barrier region where $E < v(z)$, i.e., the momentum $p(z)$ is imaginary. We take into account the absorption by introducing an imaginary part into the potential: $V(z) = v(z) - i\omega(z)$. If $\omega(z) \ll v(z)$ below the barrier, we can expand the argument of the exponential:

$$i\sqrt{2m[E-V(z)]} = -|p(z)| + i\frac{m\omega(z)}{|p(z)|} - \frac{m^2\omega^2(z)}{2|p(z)|^3} + \ldots \tag{77}$$

As usual, the first term of this expansion leads to a phase shift outside the barrier and to exponential damping below the barrier. The second term in (77) causes exponential damping (absorption) outside the barrier but only a phase shift below it.[88] Therefore below the barrier absorption occurs only in the second order in $\omega(z)$. This conclusion obviously follows from the interpretation of the tunneling as motion in imaginary time.

This quantum-mechanical effect can be manifested in a variety of phenomena, for example, in the tunneling of a light beam through a gap between walls in the case of total internal reflection, in the Josephson effect, etc.

In the case of production of a $p\bar{p}$ pair from the vacuum in a nuclear medium the term in (77) quadratic in ω leads to a small suppression of the production probability by a factor (Ref. 88) $\exp(\omega^2\gamma/\varkappa)$. Here, $\omega = \sigma\rho/2$, where $\sigma \approx 60 \times 10^{-27}$ cm^2 is the annihilation cross section, $\rho \approx 0.15$ F^{-3} is the average nuclear density, and $\gamma \approx 2.5$ is the Lorentz factor for initial momentum 10 GeV. Thus, the suppression does not exceed 10%.

It can be seen from Fig. 28 that in half of the events the $\bar{p}$ are produced outside the nucleus. For A_{eff} we can therefore write

$$A_{\text{eff}} \approx \frac{1}{2}\int d^2\mathbf{b}\int_{-\infty}^{\infty} dz\,\rho(\mathbf{b}, z)\,e^{-\sigma_{\text{in}}^{pN}T(\mathbf{b},\,-\infty,\,z)} \times\{1+e^{-\sigma_{\text{in}}^{\bar{p}N}T(\mathbf{b},\,z,\,\infty)}\} \approx \frac{1}{2}\left(\frac{\sigma_{\text{in}}^{\bar{p}A}-\sigma_{\text{in}}^{pA}}{\sigma_{\text{in}}^{\bar{p}N}-\sigma_{\text{in}}^{pN}}+\frac{\sigma_{\text{in}}^{pA}}{\sigma_{\text{in}}^{pN}}\right). \tag{78}$$

Here, the first term has an A dependence $A^{1/3}$, and the second has $A^{2/3}$. The calculation of the A dependence of the cross section in accordance with the expression (78) is compared in Fig. 29 with experimental data[90] obtained at the Institute for High Energy Physics at Serpukhov at momentum 10 GeV. The data do indeed exhibit a steep A dependence, $\sim A^{0.6}$. However, to test the specific dependence (78) we require measurements with higher accuracy, and also on a hydrogen target.

4.6. Below-threshold production of K^+ mesons on multiquark configurations in nuclei

Hadrons can be produced on nuclei at energies below the threshold for a nucleon target by means, for example, of the Fermi motion of the nuclear nucleons. However, with decreasing energy the importance of cooperative effects—the interaction of the incident hadron with a group of nuclear nucleons—must increase. Near the absolute kinematic threshold for the nucleus, all the nuclear nucleons must participate in the production process.

One of the possibilities for the cooperative phenomenon in the production of hadrons on nuclei is the interaction of the incident hadron with a group of nucleons that form a single multiquark system.[91] It will be shown below that the below-threshold production of hadrons on nuclei is sensitive to small admixtures of multiquark clusters in nuclei.[92,93]

Suppose that in a light nucleus with atomic number n there exists an admixture of a multiquark cluster with $3n$ quarks that is a quasistationary state with large mass (for example, a multiquark bag). The state of the nucleus can be described as the superposition

$$\Psi_n = \alpha_n\Psi_N + \beta_n\Psi_q. \tag{78'}$$

Here, we for the moment ignore admixtures of lighter multiquark clusters. The second coefficient is $\beta_n = U_{Nq}/\Delta E \ll 1$, where $U_{Nq} = \langle\Psi_q|\hat{H}|\Psi_N\rangle$ is the matrix element of the part of the Hamiltonian that mixes the states (78'); ΔE is the energy difference of these states. In what follows we shall assume that ΔE appreciably exceeds the binding energy of the light nuclei, as is indicated by calculations in the MIT bag model.

We consider below-threshold production of K^+ mesons

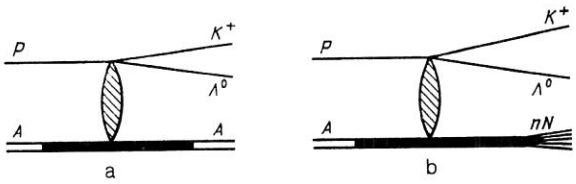

FIG. 30. Process of $K^+\Lambda^0$ production on a multiquark cluster without disintegration of the nucleus (a) and with it (b).

on multiquark clusters. We shall discuss the two possibilities shown in Fig. 30. In the first case, the nucleus does not disintegrate (Fig. 30a). We write the cross section for this process in the form

$$\sigma_n^a(T) = \beta_n^4 J_n^a(T), \tag{79}$$

where

$$J_n^a(T) = \frac{1}{v} |F_n|^2 \tau_3(W_n; m_K, m_\Lambda, M_n).$$

Here, T and v are the kinetic energy and velocity of the incident hadron; F_n is the matrix element for production of a $K^+\Lambda$ pair in a collision of a proton with a $3n$-quark cluster; and τ_3 is the three-particle phase space, which depends on W_n, the total kinetic energy of the reaction products in the center-of-mass system, and the masses of the K^+, Λ, and nuclear remnant.

We make the following assumptions about the amplitude F_n:

1) we assume that

$$|F_n|^2 \approx \frac{\sigma_{\text{in}}^{p\,\text{MQC}}}{\sigma_{\text{in}}^{pN}} |F_1|^2 \approx n^{2/3} |F_1|^2, \tag{80}$$

where F_1 is the amplitude for production of K^+ on a nucleon, and $\sigma_{\text{in}}^{p\text{MQC}}$ is the cross section for inelastic collision of the proton with the multiquark cluster. This relation can be justified in the color-tube model.

If a quark pair is to be produced, the tube must have a sufficient length in the center-of-mass system: $l \gtrsim 2m_q$, where m_q is the mass of the constituent quark, and ≈ 1 GeV/F is the energy density per unit length of the tube. It is assumed that the probability of production of an $s\bar{s}$ pair is determined solely by the tube length $l(t)$ and does not depend on the species of the interacting hadrons. The maximal length to which the color tube can be stretched depends only on the total energy release W. Therefore, the ratio of the cross sections for production of an $s\bar{s}$ pair on a multiquark cluster and on a nucleon at the same value of W is equal to the ratio $\sigma_{\text{in}}^{p\text{MQC}}/\sigma_{\text{in}}^{pN}$ of the color charge-exchange cross sections. The entire dependence of the cross section on the initial energy is determined by the phase space.

2) The concept of a color tube is meaningful if the internal momenta of the quarks in the hadrons are appreciably less than the initial momenta of the colliding hadrons. In the given case this condition is satisfied.

3) In the process of production of a K^+ meson, the recoil nucleus acquires a longitudinal momentum of about 1 GeV. If this momentum were transferred to a small fraction of the quarks in a multiquark cluster, then a form factor should also be taken into account. However, in the color-tube model the momentum is transferred "softly," during a long time. The color forces accelerate the multiquark cluster, acting on all the quarks. Therefore, a form factor should not be manifested. For a more rigorous justification of this assumption we need a definite dynamical model.

Thus, $|F_n|^2$ can be found by means of the expression (80) from data on the $pp \to K^+\Lambda_p$ reaction at energies above the threshold. To a sufficient accuracy we can set

$$J_n^a(T) = n^{2/3}\sigma_N^{K\Lambda}(T') \frac{\tau_3(W_n; m_K, m_\Lambda, M_n)}{\tau_3(W_1'; m_K, m_\Lambda, m_N)}. \tag{81}$$

Here T' is an arbitrary energy of a pp collision near the threshold at which there are data on $\sigma_N^{K\Lambda}(T')$.

The calculation of the cross section of the process with disintegration of the nucleus, which is shown in Fig. 30b, is similar. The relative contribution of the process with disintegration of the nucleus is suppressed by three orders of magnitude.[93] This occurs because the energy release is small: $W_4 \approx 0.075$ GeV.

For nuclei with $A = n$ the contribution of this mechanism of below-threshold production on a $3n$-quark cluster is not, of course, the only one. There are also contributions from lighter multiquark clusters (if the energy is not too low), a contribution of the nucleon part of the nuclear wave function due to the Fermi motion of the nucleons, and other possible mechanisms. Therefore, by comparing the expression (79) with experimental data we can obtain only an upper bound on the value of β_n^2:

$$\beta_n^4 < \sigma_n^{\text{exp}}(T)/J_n^a(T). \tag{82}$$

Unfortunately, for the lightest nuclei the necessary data are not available. However, as an estimate we can use the data of Ref. 94 for heavier nuclei.

The probability that in a nucleus with atomic number A a group of n nucleons are found in a cluster separated by relatively short distances of order $\gamma^{-1/2}$ is[92,93]

$$P_{A,n}(\mathbf{r}) = \binom{A}{n} \left(1 + \frac{\gamma n}{\delta}\right)^{-\frac{3}{2}(n-1)} \times \left(\frac{nA\delta}{\pi(A-n)}\right)^{\frac{3}{2}} \exp\left(-\frac{nA}{A-n}\delta\mathbf{r}^2\right). \tag{83}$$

In the case of a light nucleus with $A = n$ the probability for all the nucleons to come together is

$$P_n = (1 + \gamma n/\delta)^{-\frac{3}{2}(n-1)} \tag{84}$$

We must here also take into account the matrix element for the transition of a system of n colorless nucleons into a multiquark cluster. However, it is natural to assume that all these factors operate irrespective of whether or not the n nucleons belong to a heavier nucleus. In other words

$$\beta_{A,n}^2(\mathbf{r}) = \beta_n^2 P_{A,n}(\mathbf{r})/P_n. \tag{85}$$

Here, $\beta_{A,n}^2(\mathbf{r})$ is the probability of finding a cluster of $3n$ quarks at the point with coordinate $\mathbf{r}$ in the nucleus A.

Note that $\gamma n/\delta \gg 1$, since the mean square radius of the nucleus is $\langle r_A^2 \rangle = 3/2\delta^{-1}$, $\gamma = r_0^2$, where $r_0 \approx 0.5$ F is the radius of the nucleon core. With allowance for this, the dependence on γ in (85) disappears:

$$\frac{P_{A,n}(r)}{P_n} \approx \binom{A}{n} \left(\frac{\delta_A}{\delta_n}\right)^{\frac{3}{2}(n-1)} \rho^n(r) \left[\int d^3r\, \rho^n(r)\right]^{-1} \tag{86}$$

Here, $\rho(r)$ is the single-particle density of the nucleons in the

TABLE III. Upper bounds on the admixture β_n^2 of a multiquark cluster of n quarks in a nucleus with $A = n$.

n	2	3	4
$(\beta_n^2)^{\max}$	—	0.076	0.014
$(\beta_n^2)_F^{\max}$	0.06	0.015	0.008

nucleus. Note that (86) admits a transparent geometrical interpretation (cf. Ref. 95).

The cross section for K^+ production on a multiquark cluster in a heavy nucleus A is related to the cross section $\sigma_n(T)$ of K^+ production on a nucleus with $A = n$ by

$$\sigma_{A,n}(T) = \beta_n^4 J_n(T) \binom{A}{n} \left(\frac{n}{A}\right)^{n-1} I_{A,n};$$

$$I_{A,n} = \int d^2b \int_{-\infty}^{\infty} dz \exp\left[-\sigma_{\text{in}}^{NN} \int_{-\infty}^{\infty} dz' \rho(b, z')\right] \times \rho^n(b, z)\left[\int d^3\mathbf{r}\, \rho^n(\mathbf{r})\right]^{-1}, \quad (87)$$

where $J_n(T)$ is defined in (79).

If it is assumed that the cross section of K^+ production on the nucleus is completely determined by the contribution of a multiquark cluster with given n, then from comparison of the expression (87) with experimental data it is possible to find an upper limit $(\beta_n^2)^{\max}$ on the admixture of such a cluster. The results of such a comparison are given in Table III.

It can be seen from (79) and (87) that the energy dependence of the cross section $\sigma_{A,n}(T)$ is completely determined by W_n^2. The values of W_n^2 calculated at different energies for $n = 3$ and 4 are given in Fig. 31. It can be seen that W_n^2 decreases with decreasing T too rapidly compared with the energy dependence of the data.[94] This is not surprising, since we have not taken into account the Fermi motion and the binding energy of the cluster, the importance of which increases with decreasing initial energy.

Suppose that a multiquark cluster in a heavy nucleus is formed from n nucleons that have binding energies ε_i and Fermi momenta $\mathbf{k}_i$. Allowance for the Fermi motion of the cluster reduces to replacement in (87) of W_n^2 by $\langle W_n^2\rangle_F$, where

$$\langle W_n^2\rangle_F = \binom{A}{n}^{-1} \sum \int d\varepsilon\, d^3\mathbf{k} \prod_{i=1}^{n} \frac{d^3\mathbf{k}}{(2\pi)^3} |\Psi_i(\mathbf{k}_i)|^2 \times \delta\left(\varepsilon - \sum_{i=1}^{n} \varepsilon_i\right) \delta\left(\mathbf{k} - \sum_{i=1}^{n} \mathbf{k}_i\right) W_n^2(\varepsilon, \mathbf{k}). \quad (88)$$

Here, the summation is over the different ways in which the n nucleons can be chosen, and $\Psi_i(\mathbf{k})_i$ is the wave function of the corresponding level.

The results[92,93] of the averaging $\langle W_n^2\rangle_F$ for the C and Pb nuclei for different values of n and different initial energies are given in Fig. 31. Comparison with the experimental data,[94] also normalized for convenience at $T = 1$ GeV, shows that the contributions of multiquark clusters with n equal to 2, 3, 4 have an energy dependence close to the experimental one. The A dependence of the K^+ production cross section at $T = 1$ GeV is shown in Fig. 32 for n equal to 2, 3, 4. The contributions of the clusters with different n have been normalized to the experimental value of the cross section for the Pb nucleus by the selection of the factor β_n^2 in the expression (87). Note that these values $\beta_n^2 = (\beta_n^2)_F^{\max}$ are, as we have already noted, upper bounds for the cluster admixture. The corresponding values are given in Table III. It can be seen that allowance for the Fermi motion and the nucleon binding energies has appreciably influenced the value of $(\beta_n^2)^{\max}$.

Unfortunately, the interval of energies $0.84 \leqslant T \leqslant 1$ GeV does not permit any conclusions about a dominant contribution of multiquark clusters with a certain n to be drawn. In this connection it would be desirable to obtain data at lower energies, where the importance of heavy multiquark clusters must increase.

Despite the good description of the experimental data, the question of the part played by multiquark clusters in below-threshold production remains open. Nevertheless, the upper bounds β_n^2, the cluster admixture, that have been

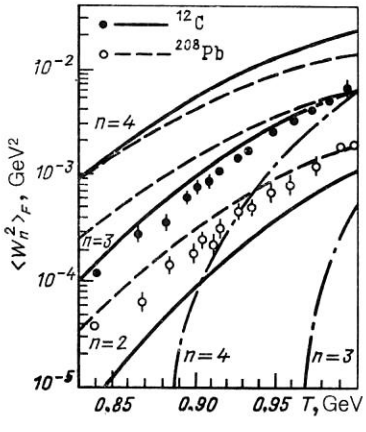

FIG. 31. Energy dependence of $\langle W_n^2\rangle_F$ for different values of n. The points are from Ref. 94 and are taken in an arbitrary normalization.

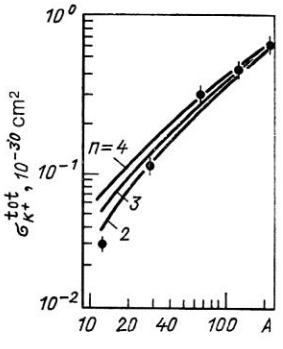

FIG. 32. The A dependence of the cross section of below-threshold K^+ production at $E_{\text{kin}} = 1$ GeV. The experimental points are the data of Ref. 94, and the curves are the contributions of multiquark clusters with different values of n, normalized to the Pb nucleus.

found correspond in order of magnitude to the estimates obtained from other processes. It may therefore be believed that the contribution of the clusters is important.

Since the probability of formation of a multiquark cluster with $I = 0(1/2)$, $S = 0(1/2)$ is suppressed in heavy nuclei, it is desirable to obtain data on the below-threshold production on the lightest nuclei with $A = n$, in which, in addition, there is no problem with the allowance for the Fermi motion.

CONCLUSIONS

It is widely believed that the inelastic corrections to the cross sections of hadron–nucleus reactions are small, readily calculated, and therefore of little interest. This may be so when one is considering the total cross sections. However, in processes with nondiagonal transitions the inelastic corrections become large and sometimes increase the cross section of a process by several times. In such cases a restriction to the inelastic corrections of first order can no longer be made, and the calculations become strongly model-dependent. But this is what makes the problem interesting, since one can test the models critically. From this point of view we have considered in this review various processes in which the corrections are large and sensitive to the predictions of QCD. The most striking manifestation of these effects is the sharp increase in the transparency of nuclei for compressed hadronic configurations, which prove the existence in hadrons of hidden color. The experimental verification of this assertion still requires great efforts. Although the comparison with the data on quasifree charge exchange made in Sec. 2 demonstrated a statistically significant effect, the result was based on a quantitative comparison, since the experiment did not separate the quasibinary kinematics and it was necessary to take into account the contribution of multiple rescatterings. Separation of single quasifree scattering on a nuclear nucleon and observation of the qualitative effect were achieved only in the reaction $\pi^+ N \to K^+ Y$, for which, unfortunately, the statistics is poor (see Fig. 8), and also in the recent experiment of Ref. 96 on quasielastic scattering of protons by nuclei through 90° in the center-of-mass system, made at energies of about 10 GeV at Brookhaven National Laboratory. Despite serious distortions due to mixing of the eigenstates (the smallness of the energy), a growth of A_{eff} with the energy was indeed observed up to 10 GeV, but on the interval 10–12 GeV the value of A_{eff} decreased noticeably. This last result, which has not yet been satisfactorily explained, prevents us from regarding the results of the experiment as convincing. Measurements at higher energies are needed. It is also necessary to study the A dependence of the cross section for quasifree charge exchange $\pi^+ n \to \pi^0(\eta^0) p$ on nuclear neutrons with detection of the recoil proton, for which, as was found, much lower momentum transfers than in quasielastic scattering are needed.

In our study of the space–time picture of the hadronization of colored objects we assumed that in a nuclear medium this process takes place in the same way as in the vacuum. This assumption may not be valid. Indeed, in the model of a color tube, as we showed in the Introduction, the tube parameters (transverse section, tension coefficient, probability of production of quark–antiquark pairs) depend strongly on the discontinuity of the vacuum energy density at the surface that bounds the tube. From the point of view of the bag model, the nuclear medium is filled with nucleon "bubbles," within which the energy density is below the vacuum value in absolute magnitude. For this reason the parameters of a color tube formed by the separation of color charges within a nucleus can change, and therefore the course of the hadronization process can change as well. Nevertheless, these corrections are quantitatively small. Indeed, comparison of the known values of the vacuum energy density and the constant B of the bag model shows[66] that the energy density within a bag is suppressed by only 5–10% compared with the vacuum value. For the energy density averaged over the nucleus this difference is even less. Thus, one could think that there will be no radical change of the process of hadronization of color charges within a nucleus.

In the framework of this assumption, it is possible to use the nuclear medium to analyze the space–time picture of the hadronization process. In order to draw a reliable conclusion about the dynamics of a process using only the A dependences of various characteristics it is necessary to make a special choice of the reaction and the kinematic region in which the effects in which we are interested are enhanced. Examples of this kind given in the review provide serious arguments for the hypothesis of soft color screening in the process of hadronization of colored objects. Nevertheless, we require a comprehensive study at different energies of the processes considered here, such as inclusive production of hadrons in hA collisions in the limit $x_F \to 1$, the x_F dependence of the cross section for production on nuclei of lepton pairs with large mass, the A dependence of the cross section for production of symmetric pairs of hadrons with large x_T, and below-threshold production of K^+ mesons and $\bar{p}$ at lower energies. This list may be significantly extended by new assumptions, but unfortunately this could not be done in the framework of the present paper.

I should like to express my sincere gratitude to A. V. Efremov for a number of valuable comments on the content of the review.

[1)] From this we see the naivety of the attempts found in the literature to obtain free color charges by lowering the potential barrier at large distances. The probability of separating charges to such distances without producing pairs, i.e., without screening the charges, is negligibly small. This conclusion is a general result of quantum mechanics, and not merely of the string model.

[2)] In Ref. 50 the corrections to the cross section for pd scattering in the constituent-quark model were considered without allowance for the Pomeron color structure. The corrections were found to be small.

[1] R. J. Glauber, *Lectures in Theoretical Physics*, Vol. 1 (Interscience, New York, 1959), p. 315.
[2] O. G. Sitenko, Ukr. Fiz. Zh. **4**, 152 (1959).
[3] N. N. Nikolaev, Usp. Fiz. Nauk **134**, 369 (1981) [Sov. Phys. Usp. **24**, 531 (1981)]; Fiz. Elem. Chastits At. Yadra **12**, 162 (1981) [Sov. J. Part. Nucl. **12**, 63 (1981)].
[4] Yu. M. Shabel'skiĭ, Fiz. Elem. Chastits At. Yadra **12**, 1070 (1981) [Sov. J. Part. Nucl. **12**, 430 (1981)].
[5] V. N. Gribov, Zh. Eksp. Teor. Fiz. **56**, 892 (1969) [Sov. Phys. JETP **29**, 483 (1969)].
[6] J. Pumplin and M. Ross, Phys. Rev. Lett. **21**, 1778 (1968).
[7] V. V. Anisovich, P. E. Volkovitsky and L. G. Dakhno, Phys. Lett. **42B**, 224 (1972).
[8] A. B. Kaĭdalov and L. A. Kondratyuk, Pis'ma Zh. Eksp. Teor. Fiz. **15**, 170 (1972) [JETP Lett. **15**, 117 (1972)].
[9] V. V. Anisovich and L. G. Dakhno, Nucl. Phys. **B85**, 208 (1975); L. G. Dakhno, Yad. Fiz. **37**, 993 (1983) [Sov. J. Nucl. Phys. **37**, 590 (1983)].
[10] V. A. Karmanov and L. A. Kondratyuk, Pis'ma Zh. Eksp. Teor. Fiz. **18**, 451 (1973) [JETP Lett. **18**, 266 (1973)].
[11] O. V. Kancheli, Pis'ma Zh. Eksp. Teor. Fiz. **18**, 465 (1973) [JETP Lett. **18**, 274 (1973)].

[12]P. V. R. Murthy, C. A. Ayre, H. R. Gustafson *et al.*, Nucl. Phys. **B92**, 269 (1975).
[13]A. Gsponer, J. Hoffnagle, W. R. Molzon *et al.*, Phys. Rev. Lett. **42**, 9 (1979).
[14]N. N. Nikolaev, Zh. Eksp. Teor. Fiz. **81**, 814 (1981) [Sov. Phys. JETP **54**, 434 (1981)].
[15]N. N. Nikolaev, INS-Rep.-538, Tokyo (1985).
[16]E. L. Feinberg and I. Ya. Pomeranchuk, Nuovo Cimento Suppl. **3**, 652 (1956).
[17]M. L. Good and W. D. Walker Phys. Rev **120**, 1857 (1960).
[18]P. G. Grassberger, Nucl. Phys. **B125**, 83 (1977).
[19]H. I. Miettinen and J. Pumplin, Phys. Rev. D **18**, 1696 (1978).
[20]B. Z. Kopeliovich and L. I. Lapidus, in *Proc. of the Fifth International Seminar on Multiparticle Production of Hadrons at High Energies* [in Russian] (Dubna, 1978), p. 469.
[21]B. Z. Kopeliovich and L. I. Lapidus, Pis'ma Zh. Eksp. Teor. Fiz. **28**, 664 (1978) [JETP Lett. **28**, 595 (1978)].
[22]C. W. De Jager, H. De Vries, and C. De Vries, Nucl. Data Tables **14**, 479 (1974).
[23]B. Z. Kopeliovich and L. I. Lapidus, Pis'ma Zh. Eksp. Teor. Fiz. **32**, 612 (1980) [JETP Lett. **32**, 597 (1980)]; L. Rosen, in *High Energy and Nuclear Structure*, edited by D. E. Nagle (AIP, New York, 1975).
[24]V. L. Lyuboshits and M. I. Podgoretskiĭ, Zh. Eksp. Teor. Fiz. **81**, 1556 (1981) [Sov. Phys. JETP **54**, 827 (1981)].
[25]F. Low, Phys. Rev. D **12**, 163 (1975).
[26]S. Nussinov, Phys. Rev. Lett. 34 1286 (1975).
[27]Y. F. Gunion and H. Soper, Phys. Rev. D **15**, 2617 (1977).
[28]E. M. Levin and M. G. Ryskin, Yad. Fiz. **34**, 1114 (1981) [Sov. J. Nucl. Phys. **34**, 619 (1981)].
[29]A. B. Zamolodchikov, B. Z. Kopeliovich, and L. I. Lapidus, Pis'ma Zh. Eksp. Teor. Fiz. **33**, 612 (1981) [JETP Lett. **33**, 595 (1981)].
[30]J. Bertch, S. J. Brodsky, A. S. Goldhaber, and J. G. Gunion, Phys. Rev. Lett. **47**, 297 (1981).
[31]B. Z. Kopeliovich, in *Proc. of the 13th Winter School of the Institute of High Energy Physics, Serpukhov*, Vol. 1 [in Russian] (Énergoatomizdat, Moscow, 1986), p. 3.
[32]A. V. Tarasov, Fiz. Elem. Chastits At. Yadra **7**, 771 (1976) [Sov. J. Part. Nucl. **7**, 306 (1975)].
[33]A. B. Zamolodchikov, B. Z. Kopeliovich, and L. I. Lapidus, Yad. Fiz. **35**, 129 (1982) [Sov. J. Nucl. Phys. **35**, 75 (1982)].
[34]A. Gsponer, Phys. Rev. Lett. **42**, 13 (1979).
[35]B. Z. Kopeliovich and N. N. Nikolaev, Z. Phys. C **5**, 333 (1980).
[36]B. Z. Kopeliovich, in *Materials of the 19th Winter School of the Leningrad Institute of Nuclear Physics* [in Russian] (Leningrad, 1984), p. 169.
[37]B. G. Zakharov and B. Z. Kopeliovich, Yad. Fiz. **46**, 1535 (1987) [Sov. J. Nucl. Phys. **46**, 911 (1987)].
[38]V. V. Anisovich and V. M. Braun, Preprint LNPI 732, Leningrad (1982).
[39]A. H. Mueller, CU-TP-232, Columbia University, New York (1982).
[40]W. D. Apel, K. H. Augenstein, E. Bertolucci *et al.*, Nucl. Phys. **B152**, 1 (1979).
[41]V. D. Apokin, A. N. Vasil'ev, Yu. A. Matulenko *et al.*, Yad. Fiz. **36**, 1191 (1982) [Sov. J. Nucl. Phys. **36**, 694 (1982)].
[42]P. D. B. Collins, *An Introduction to Regge Theory and High-Energy Physics* (Cambridge University Press, Cambridge, 1977) [Russ. transl., Atomizdat, Moscow, 1980].
[43]V. V. Anisovich, M. N. Kobrinsky, V. A. Nikonov, Int. J. Mod. Phys. **A1**, 463 (1986).
[44]G. S. Bitsadze, Yu. A. Budagov, V. P. Dzhelepov *et al.*, Communication E1-86-780, JINR, Dubna (1986).
[45]Yu. M. Kazarinov B. Z. Kopeliovich, L. I. Lapidus, and I. K. Potashnikova, Zh. Eksp. Teor. Fiz. **70**, 1152 (1976) [Sov. Phys. JETP **43**, 598 (1976)].
[46]B. Z. Kopeliovich and N. A. Rusakovich, Communication E2-86-298, JINR, Dubna (1986).
[47]G. S. Bitsadze *et al.*, Nucl. Phys. **B279**, 770 (1987).
[48]B. Z. Kopeliovich and B. G. Zakharov, Z. Phys. C **26**, 459 (1984).
[49]B. G. Zakharov and B. Z. Kopeliovich, Yad. Fiz. **42**, 1073 (1985) [Sov. J. Nucl. Phys. **42**, 677 (1985)].
[50]B. G. Zakharov, Pis'ma Zh. Eksp. Teor. Fiz. **36**, 412 (1982) [JETP Lett. **36**, 500 (1982)].
[51]V. A. Khoze *et al.*, Nucl. Phys. **B124**, 539 (1977).
[52]A. P. Kobushkin, Yad. Fiz. **28**, 495 (1978) [Sov. J. Nucl. Phys. **28**, 252 (1978)].
[53]A. Th. Aerts, P. J. G. Mulders, and J. J. De Swart, Phys. Rev. D **17**, 260 (1978); I. T. Obukhovskiĭ and E. V. Tkalya, Yad. Fiz. **35**, 288 (1982) [Sov. J. Nucl. Phys. 35, 164 (1982)].
[54]I. T. Obukhovskiĭ, Yad. Fiz. **37**, 27 (1983) [Sov. J. Nucl. Phys. **37**, 15 (1983)].
[55]B. Z. Kopeliovich and F. Niedermayer, Phys. Lett. **117B**, 101 (1982).
[56]B. Z. Kopeliovich and F. Niedermayer, Zh. Eksp. Teor. Fiz. **87**, 1121 (1984) [Sov. Phys. JETP **60**, 640 (1984)].
[57]B. Z. Kopeliovich and F. Niedermayer, Communication E2-84-786, JINR, Dubna (1984).
[58]A. Casher, H. Neuberger, and S. Nussinov, Phys. Rev. D **20**, 179 (1979).
[59]E. Gurvich, Phys. Lett. **87B**, 386 (1979).
[60]E. G. Gurvich, Pis'ma Zh. Eksp. Teor. Fiz. **32**, 491 (1980); **41**, 358 (1985) [JETP Lett. **32**, 471 (1980); **41**, 439 (1985)].
[61]B. Z. Kopeliovich, Yad. Fiz. **26**, 168 (1977) [Sov. J. Nucl. Phys. **26**, 87 (1977)].
L. L. Frankfurt and M. I. Strikman, Phys. Rep. **76**, 215 (1981).
[63]A. M. Baldin, V. K. Bondarev, V. L. Mazarskiĭ *et al.*, Communication Rl-11168 [in Russian], JINR, Dubna (1977); Communication Rl-80-488 [in Russian], JINR, Dubna (1980); A. M. Baldin, Fiz. Elem. Chastits At. Yadra **8**, 429 (1977) [Sov. J. Part. Nucl. **8**, 175 (1977)].
[64]P. Berthet, R. Frascaria, H. P. Combes *et al.*, J. Phys. G **8**, L111 (1982).
[65]K. Johnson and C. B. Thorn, Phys. Rev. D **13**, 1934 (1976).
[66]V. A. Novikov, M. A. Shifman, A. I. Vainshtein, and V. I. Zakharov, Nucl. Phys. **B191**, 301 (1981).
[67]B. Z. Kopeliovich, in *Materials of the 20th Winter School of the Leningrad Institute of Nuclear Physics* [in Russian], (Leningrad, 1985), p. 140.
[68]B. Z. Kopeliovich and F. Niedermayer, Communication E2-84-834, JINR, Dubna (1984).
[69]Yu. M. Antipov, V. A. Bessubov, N. P. Budanov *et al.*, Phys. Lett. **76B**, 235 (1978).
[70]K. J. Andersson, Phys. Rev. Lett. **42**, 944 (1979).
[71]M. J. Gorden, J. D. Dowell, J. Carvey *et al.*, Phys. Lett. **110B**, 415 (1982).
[72]J. Badier, J.Bourotte *et al.*, Z. Phys. C **20**, 101 (1983).
[73]W. Katsanevas *et al.*, E-537 Collaboration, FERMILAB-Pub.-87/57-E (1987).
[74]N. N. Nikolaev and V. R. Zoller, Nucl. Phys. **B147**, 336 (1979).
[75]B. Z. Kopeliovich and L. I. Lapidus, in *Proc. of the Sixth Balaton Conference on Nuclear Physics* (Balatonfured, Hungary, 1983), p. 73.
[76]J. W. Cronin, H. J. Frisch, M. J. Shochet *et al.*, Phys. Rev. D **11**, 3105 (1975).
[77]V. R. Zoller, N. N. Nikolaev, and A. Ya. Ostapchuk, *Sixth Physics School of the Institute of Theoretical and Experimental Physics, Serpukhov*, Part 3 [in Russian] (Atomizdat, Moscow, 1979), p. 3.
[78]R. L. McCarthy, Phys. Rev. Lett. **40**, 213 (1978).
[79]V. V. Abramov, A. M. Baldin, A. F. Buzulukov *et al.*, Communication 84-143 [in Russian], Institute of High Energy Physics, Serpukhov (1984).
[80]V. V. Abramov, A. M. Baldin, A. F. Buzulukov *et al.*, Communication 84-12 [in Russian], Institute of High Energy Physics, Serpukhov (1984).
[81]V. V. Abramov, A. M. Baldin, A. F. Buzulukov *et al.*, Communication 84-26 [in Russian], Institute of High Energy Physics, Serpukhov (1984).
[82]D. A. Finley *et al.*, Phys. Rev. Lett. **42**, 1031 (1979).
[83]Y. B. Hsiung *et al.*, Phys. Rev. Lett. **55**, 457 (1985).
[84]E605 Collaboration, FERMILAB-Rep. (1987).
[85]B. T. Kim and B. Z. Kopeliovich, Communication E2-89-727, JINR. Dubna (1989).
[86]V. A. Abramovskiĭ and O. V. Kancheli, Pis'ma Zh. Eksp. Teor. Fiz. **31**, 566 (1980) [JETP Lett. **31**, 532 (1980)].
[87]D. A. Barton, Phys. Rev. D **27**, 2580 (1983).
[88]B. Z. Kopeliovich and F. Niedermayer, Phys. Lett. **151B**, 437 (1985).
[89]V. G. Grishin, G. I. Kopylov, and M. I. Podgoretskiĭ, Yad. Fiz. **13**, 1116 (1971) [Sov. J. Nucl. Phys. **13**, 638 (1971)].
[90]A. O. Vaisenberg, O. K. Egorov, V. F. Kuzichev *et al.*, Pis'ma Zh. Eksp. Teor. Fiz. **29**, 719 (1979) [JETP Lett. **29**, 661 (1979)].
[91]V. K. Luk'yanov and A. I. Titov, Fiz. Elem. Chastits At. Yadra **10**, 815 (1979) [Sov. J. Part. Nucl. **10**, 321 (1979)].
[92]B. Z. Kopeliovich and P. Niedermayer, Phys. Rev. C **33**, 2070 (1986).
[93]B. Z. Kopeliovich and F. Niedermayer, Yad. Fiz. **44**, 517 (1986) [Sov. J. Nucl. Phys. **44**, 333 (1986)].
[94]N. K. Abrosimov, V. A. Volchenkov, A. B. Gridnev *et al.*, Pis'ma Zh. Eksp. Teor. Fiz. **36**, 211 (1982) [JETP Lett. **36**, 261 (1982)]; Preprint No. 1146 [in Russian], Leningrad Institute of Nuclear Physics, Leningrad (1985).
[95]A. V. Efremov, Fiz. Elem. Chastits At. Yadra **13**, 611 (1982) [Sov. J. Part. Nucl. **13**, 254 (1982)].

Translated by Julian B. Barbour